infection and stored at −80°C after filtering through a 0.45 μm filter (Kurabo, Osaka, Japan) until use. For infection experiments with HCV-JFH1 virus, RSc cells (1×10^5 cells/well) were plated onto 6-well plates and cultured for 24 hours (hrs). Then, we infected the cells with 50 μl (equivalent to a multiplicity of infection [MOI] of 0.1) of inoculum. The culture supernatants were collected and the levels of HCV Core were determined by enzyme-linked immunosorbent assay (ELISA) (Mitsubishi Kagaku Bio-Clinical Laboratories, Tokyo, Japan). Total RNA was isolated from the infected cellular lysates using RNeasy mini kit (Qiagen, Hilden, Germany) for quantitative RT-PCR analysis of intracellular HCV RNA. The infectivity of HCV in the culture supernatants was determined by a focus-forming assay at 48 hrs post-infection. The HCV infected cells were detected using anti-HCV Core antibody (CP-9 and CP-11). Intracellular HCV infectivity was determined by a focus-forming assay at 48 hrs post-inoculation of lysates by repeated freeze and thaw cycles (three times).

Quantitative RT-PCR Analysis

The quantitative RT-PCR analysis for HCV RNA was performed by real-time LightCycler PCR (Roche) as described previously [17,18]. We used the following forward and reverse primer sets for the real-time LightCycler PCR: TSG101, 5′-ATGGCGGTGTCGGAGAGCCA-3′ (forward), 5′-AACAGGTTTGAGATCTTTGT-3′ (reverse); Alix, 5′-ATGGCGACATTCATCTCGGT-3′ (forward), 5′-TACTGGGCCTGCTCTTCCCC-3′ (reverse); Vps4B, 5′-ATGTCATCCACTTCGCCCAA-3′ (forward), 5′-ATACTGCACAGCATGCTGAT-3′ (reverse); CHMP4b, 5′-ATGTCGGTGTTCGGGAAGCT-3′ (forward), 5′-ATCTCTTCCGTGTCCCGCAG-3′ (reverse); Brox, 5′-ATGACCCATTGGTTTCATAG-3′ (forward), 5′-CCTGGATGACCTCAAGTCAT-3′ (reverse); β-actin, 5′-TGACGGGGTCACCCACACTG-3′ (forward), 5′-AAGCTGTAGCCGCGCTCGGT-3′ (reverse); and HCV-JFH1, 5′-AGAGCCATAGTGGTCTGCGG-3′ (forward), 5′-CTTTCGCAACCCAACGCTAC-3′ (reverse).

MTT Assay

Cells (5×10^3 cells/well) were plated onto 96-well plates and cultured for 24, 48 or 72 hrs, then, subjected to the colorimetric 3-(4,5-dimethylthiazol-2-yl)-2,5-diphenyltetrazolium bromid (MTT) assay according to the manufacturer's instructions (Cell proliferation kit I, Roche). The absorbance was read using a microplate reader (Multiskan FC, Thermo Fisher Scientific) at 550 nm with a reference wavelength of 690 nm.

Renilla Luciferase (RL) Assay

OR6 cells (1.5×10^4 cells/well) [17,18] were plated onto 24-well plates and cultured for 24 hrs. The cells were transfected with siRNAs (50 nM) using Oligofectamine and incubated for 72 hrs, then, subjected to the RL assay according to the manufacturer's instructions (Promega, Madison, WI). A lumat LB9507 luminometer (Berthold, Bad Wildbad, Germany) was used to detect RL activity.

Western Blot Analysis

Cells (2×10^5 cells/well) were plated onto 6-well plates and cultured for 24 or 48 hrs. Cells were lysed in buffer containing 50 mM Tris-HCl (pH 8.0), 150 mM NaCl, 4 mM EDTA, 1% NP-40, 0.1% sodium dodecyl sulfate (SDS), 1 mM dithiothreitol (DTT) and 1 mM phenylmethylsulfonyl fluoride (PMSF). Supernatants from these lysates were subjected to SDS-polyacrylamide gel electrophoresis, followed by immunoblot analysis using anti-TSG101 antibody (BD Transduction Laboratories, San Jose, CA), anti-Alix antibody, anti-Vps4B antibody (Abnova, Taipei, Taiwan) (A302-078A; Bethyl Laboratories, Montgomery, TX), anti-CHMP4B antibody (sc-82557; Santa Cruz Biotechnology, Santa Cruz, CA), anti-HCV Core antibody, anti-β-actin antibody (Sigma), anti-Myc-Tag antibody, anti-FLAG antibody (M2; Sigma), anti-Chk2 antibody (DCS-273; MBL), anti-heat shock protein (HSP) 70 antibody (BD), Living Colors A.v. monoclonal antibody (JL-8; Clontech, Mountain View, CA), anti-HCV NS5A monoclonal antibody (no. 8926; a generous gift from A Takamizawa, The Research Foundation for Microbial Diseases of Osaka University, Japan), or anti-HCV NS5A polyclonal antibody (a generous gift from K Shimotohno, Chiba Institute of Technology, Chiba, Japan).

Immunoprecipitation Analysis

Cells were lysed in buffer containing 10 mM Tris-HCl (pH 8.0), 150 mM NaCl, 1% NP-40, 1 mM PMSF, and protease inhibitor cocktail containing 104 μM 4-(2-aminoethyl)benzenesulfonyl fluoride hydrochloride, 80 nM aprotinin, 2.1 μM leupeptin, 3.6 μM bestatin, 1.5 μM pepstatin A, and 1.4 μM E-64 (Sigma). Lysates were pre-cleaned with 30 μl of protein-G-Sepharose (GE Healthcare Bio-Sciences). Pre-cleaned supernatants were incubated with 5 μl of Living Colors A.v. monoclonal antibody or anti-FLAG antibody at 4°C for 1 hr. Following absorption of the precipitates on 30 μl of protein-G-Sepharose resin for 1 hr, the resin was washed four times with 700 μl lysis buffer. Proteins were eluted by boiling the resin for 5 min in 1× Laemmli sample buffer. The proteins were then subjected to SDS-PAGE, followed by immunoblotting analysis using either anti-FLAG antibody, Living Colors A.v. monoclonal antibody or anti-HCV Core antibody.

Statistical Analysis

Statistical comparison of the infectivity of HCV in the culture supernatants between the knockdown cells and the control cells was performed using the Student's *t*-test. *P* values of less than 0.05 were considered statistically significant. All error bars indicate standard deviation.

Results

The ESCRT system is required for HCV production

To investigate the potential role(s) of the ESCRT system in the HCV life cycle, we first used lentiviral vector-mediated RNA interference to stably knockdown the ESCRT components, including TSG101, Alix, Vps4B, or CHMP4b in HuH-7-derived RSc cured cells that cell-culture-generated HCVcc (HCV-JFH1, genotype 2a) [13] could infect and effectively replicate [14–16]. We used puromycin-resistant pooled cells 10 days after the lentiviral transduction in all experiments. Western blot and real-time LightCycler RT-PCR analyses for TSG101, Alix, Vps4B, or CHMP4b demonstrated a very effective knockdown of each ESCRT component in RSc cells transduced with lentiviral vectors expressing the corresponding shRNAs (Fig. 1A–E). Importantly, we noticed that the depletion of ESCRT components did not affect the levels of several cellular proteins, including HSP70, Chk2, and b-actin (Fig. 1A). To test the cell toxicity of each shRNA, we examined colorimetric MTT assay. In this context, we demonstrated that the shRNAs did not affect the cell viabilities (Fig. 1F). We next examined the levels of HCV Core and the infectivity of HCV in the culture supernatants as well as the level of HCV RNA in the TSG101, Alix, Vps4B, or CHMP4b stable knockdown RSc cells 97 h after HCV-JFH1 infection at an MOI of 0.1. The results showed that the release of HCV Core into the culture supernatants

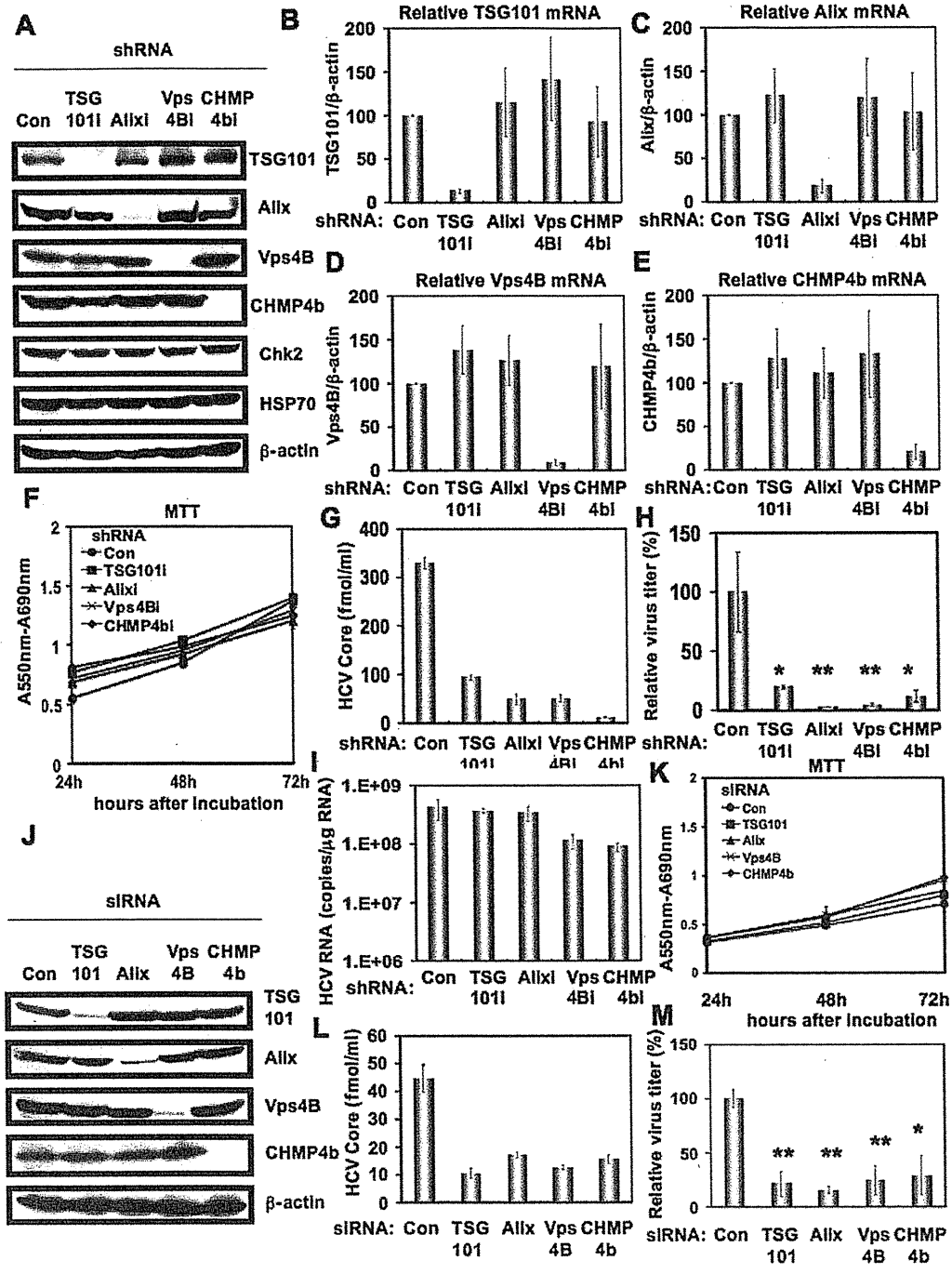

Figure 1. ESCRT components are required for the infectious HCV production. (A) Inhibition of TSG101, Alix, Vps4B, or CHMP4b protein expression by shRNA-producing lentiviral vectors. The results of the Western blot analysis of cellular lysates with anti-TSG101, anti-Alix, anti-Vps4B, anti-CHMP4b, anti-Chk2, anti-HSP70, or anti-β-actin antibody in RSc cells expressing shRNA targeted to TSG101 (TSG101i), Alix (Alixi), Vps4B (Vps4Bi), or CHMP4b (CHMP4bi) as well as in RSc cells transduced with a control lentiviral vector (Con) are shown. Real-time LightCycler RT-PCR for TSG101 (B), Alix (C), Vps4B (D), or CHMP4b mRNA (E) was performed as well as for β-actin mRNA in triplicate. Each mRNA level was calculated relative to the level in RSc cells transduced with a control lentiviral vector (Con) which was assigned as 100%. Error bars in this panel and other figures indicate standard deviations. (F) MTT assay of each knockdown RSc cells at the indicated time. (G) The levels of HCV Core in the culture supernatants from the stable knockdown RSc cells 97 h after inoculation of HCV-JFH1 at an MOI of 0.1 were determined by ELISA. Experiments were done in triplicate and columns represent the mean Core protein levels. (H) The infectivity of HCV in the culture supernatants from the stable knockdown RSc cells 97 hrs after inoculation of HCV-JFH1 at an MOI of 0.1 was determined by a focus-forming assay at 48 hrs post-infection. Experiments were done in triplicate and each virus titer was calculated relative to the level in RSc cells transduced with a control lentiviral vector (Con) which was assigned as 100%. Asterisks indicate significant differences compared to the control treatment. *$P<0.05$; **$P<0.01$. (I) The level of intracellular genome-length HCV-JFH1 RNA in the cells at 97 hrs post-infection was monitored by real-time LightCycler RT-PCR. Results

from three independent experiments are shown. (J) Inhibition of TSG101, Alix, Vps4B, or CHMP4b protein expression by 72 hrs after transient transfection of RSc cells with a pool of control siRNA (Con) or a pool of siRNA specific for Alix, Vps4B, or CHMP4b (50 nM). The results of the Western blot analysis of cellular lysates with anti-TSG101, anti-Alix, anti-Vps4B, anti-CHMP4b, or anti-β-actin antibody is shown. (K) MTT assay of each knockdown RSc cells at the indicated time. (L) The levels of HCV Core in the culture supernatants were determined by ELISA 24 hrs after inoculation of HCV-JFH1. RSc cells were transiently transfected with a pool of control siRNA (Con) or a pool of siRNA specific for TSG101, Alix, Vps4B, or CHMP4b (50 nM). At 48 hrs after transfection, the cells were inoculated with HCV-JFH1 at an MOI of 5 and incubated for 2 hrs. Then, culture medium was changed and incubated for 22 hrs. Experiments were done in triplicate and each Core level was calculated relative to the level in the culture supernatants from the control cells and indicated below. (M) The infectivity of HCV in the culture supernatants from the transient knockdown RSc cells 24 hrs after inoculation of HCV-JFH1 at an MOI of 5 was determined by a focus-forming assay at 48 hrs post-infection. Experiments were done in triplicate and each virus titer was calculated relative to the level in RSc cells transfected with a control siRNA (Con) which was assigned as 100%. Asterisks indicate significant differences compared to the control treatment. *$P<0.05$; **$P<0.01$.

doi:10.1371/journal.pone.0014517.g001

was significantly suppressed in these knockdown cells after HCV-JFH1 infection (Fig. 1G). Importantly, the infectivity of HCV in the culture supernatants was also significantly suppressed in these knockdown cells (Fig. 1H), while the RNA replication of HCV-JFH1 was not affected in the TSG101 or Alix knockdown cells and was somewhat decreased in the Vps4B and CHMP4b knockdown cells (Fig. 1I). This suggested that the ESCRT system is associated with infectious HCV production. To further confirm whether or not the ESCRT system is involved in HCV production, we analyzed the single-round HCV replication. For this, we used RSc cells transiently transfected with a pool of siRNAs specific for TSG101, Alix, Vps4B, or CHMP4b as well as a pool of control siRNAs (Con) following HCV infection. In spite of very effective knockdown of each ESCRT component (Fig. 1J), we demonstrated that the siRNAs did not affect the cell viabilities by MTT assay (Fig. 1K). Consistent with our finding using the stable knockdown cells, we observed that the release of HCV Core or the infectivity of HCV into the culture supernatants was significantly suppressed in these transient knockdown cells 24 hrs after HCV-JFH1 infection (Fig. 1L and 1M). Furthermore, we examined the effect of siRNA specific for TSG101, Alix, Vps4B, or CHMP4b in HCV RNA replication using the subgenomic JFH1 replicon, JRN/3-5B, encoding *Renilla* luciferase gene for monitoring the HCV RNA replication in HuH-7-derived OR6c JRN/3-5B cells (Fig. 2A and 2B) or an OR6 assay system, which was developed as a luciferase reporter assay system for monitoring genome-length HCV RNA replication (HCV-O, genotype 1b) in HuH-7-derived OR6 cells (Fig. 2C) [17,18]. The results showed that these siRNAs could not affect HCV RNA replication as well as the levels of intracellular NS5A proteins (Fig. 2A–C). Although we have demonstrated that the ESCRT system is required for production of extracellular infectious HCV particles, it is not clear whether or not these findings are associated with the assembly of intracellular infectious particles. To test this point, infectivity of intracellular infectious particles was analyzed following lysis of HCV-JFH1-infected knockdown cells by repetitive freeze and thaw. Consequently, we did not observe any significant effects of siRNAs on the accumulation of intracellular infectious HCV-JFH1, while the accumulation of extracellular HCV was significantly suppressed in these knockdown cells (Fig. 2D and 2E), indicating that inhibition of the ESCRT system does not block the accumulation of intracellular infectious HCV particles. Furthermore, Western blot analysis of cell lysates demonstrated that the level of intracellular HCV Core and NS5A was not affected in these knockdown cells 72 hrs post-infection (Fig. 2F). Thus, we conclude that the ESCRT system is not required for the assembly of infectious particles but the ESCRT system is required for late step of HCV production.

HCV Core can target into lipid droplets in the ESCRT knockdown cells

Since lipid droplets have been shown to be involved in an important cytoplasmic organelle for HCV production [4], we performed immunofluorescence and confocal microscopic analyses to determine whether or not HCV Core misses localization into lipid droplets in the ESCRT knockdown cells. We found that the Core was targeted into lipid droplets even in TSG101 knockdown, Alix knockdown, Vps4B knockdown, or CHMP4b knockdown RSc cells as well as in the control RSc cells after HCV infection (Fig. 3). This suggests that the ESCRT system plays a role in the late step after the Core is targeted into lipid droplets in the HCV life cycle.

HCV Core interacts with CHMP4b

To determine whether or not HCV Core can interact with ESCRT component(s), we examined their subcellular localization by confocal laser scanning microscopy. Consequently, the Core mostly colocalized with CHMP4b-green fluorescent protein (GFP) or FLAG-tagged CHMP4b in the perinuclear region of 293FT cells coexpressing them (Fig. 4A and 4B), while the CHMP4b-GFP alone was slightly diffused in the cytoplasm (Fig. 4A), indicating the recruitment of CHMP4b in the Core-expressing area. Importantly, we observed similar partial colocalization in HCV-JFH1-infected RSc cells expressing CHMP4b-GFP (Fig. 4C), whereas the CHMP4b-GFP alone was diffused in the cytoplasm in the uninfected RSc cells (Fig. 4C), suggesting the interaction of HCV Core with CHMP4b. Unfortunately, we failed to observe endogenous CHMP4b using several commercially available anti-CHMP4b antibody (data not shown). Consistent with a previous report that interaction between HCV Core and NS5A is critical for HCV production [3], we found the partial colocalization of NS5A with CHMP4b-GFP as well as the colocalization of Core with CHMP4b-GFP in HCV-JFH1-infected RSc cells (Fig. 4C). Then, we examined whether or not HCV Core can bind to CHMP4b by immunoprecipitation analysis. 293FT cells transfected with 4 mg of pCHMP4b-GFP, pEGFP C3 (Clontech), pcDNA3-FLAG [19], pcDNA3-FLAG-Alix or pFLAG-CHMP4b and RSc cells 5 days after inoculation of HCV-JFH1 at an MOI of 4 were lysed and performed immunoprecipitation of lysate mixtures of HCV-JFH1-infected RSc cells and 293FT cells expressing CHMP4b-GFP, GFP alone, FLAG-CHMP4b or FLAG-epitope alone with anti-FLAG or anti-GFP antibody. Consequently, we observed that the Core but not the NS5A could bind to FLAG-CHMP4b (Fig. 4D). However, the Core was not immunoprecipitated with anti-FLAG antibody using the lysate mixtures of HCV-JFH1-infected RSc cell lysates and 293FT cells expressing FLAG-epitope alone or FLAG-Alix (Fig. 4D). Furthermore, the Core was coimmunoprecipitated with CHMP4b-GFP but not GFP when lysate mixtures of HCV-JFH1-infected RSc cells and 293FT cells expressing CHMP4b-GFP or GFP alone were used (Fig. 4D). In contrast, we failed to observe the marked colocalization of HCV-JFH1 Core with Myc-tagged TSG101 in HCV-JFH1-infected RSc cells expressing Myc-TSG101 or endogenous Alix in HCV-JFH1-infected RSc cells (Fig. 5A). Thus, we concluded that the HCV Core was associated with CHMP4b.

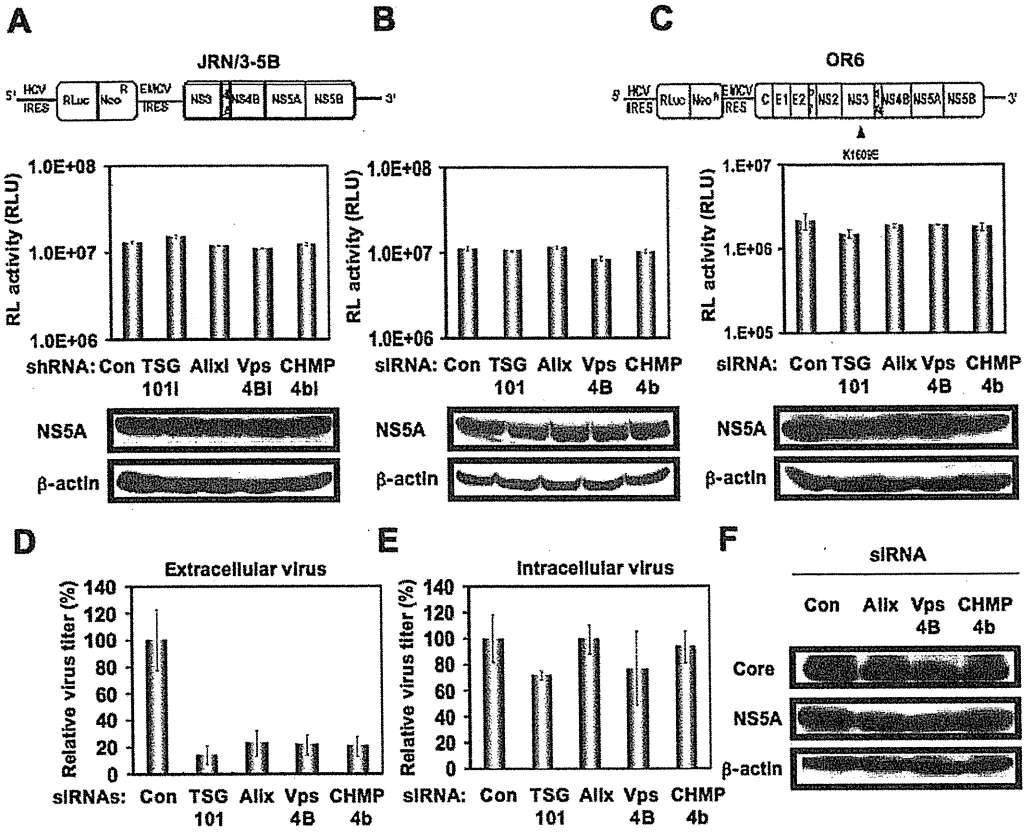

Figure 2. ESCRT system is not required for HCV RNA replication and assembly of intracellular infectious HCV. (A) Schematic gene organization of subgenomic JFH1 (JRN/3-5B) RNA encoding *Renilla* luciferase gene. Renilla luciferase gene (RLuc) is depicted as a box and is expressed as a fusion protein with Neo. The HCV RNA replication level in each ESCRT knockdown OR6c JRN/3-5B cells by lentiviral vector-mediated RNA interference (shRNA) was monitored by RL assay. The RL activity (RLU) is shown. The results shown are means from three independent experiments. (B) 72 hrs after the transfection of OR6c JRN/3-5B polyclonal cells with each of the siRNA (50 nM), the HCV RNA replication level was monitored by RL assay as described in (A). (C) Schematic gene organization of genome-length HCV-O RNA encoding *Renilla* luciferase gene. The position of an adaptive mutation, K1609E, is indicated by a triangle. 72 hrs after the transfection of OR6 cells with each of the siRNA (50 nM), the HCV RNA replication level was monitored by RL assay as described in (A). (D) The infectivity of HCV in the culture supernatants from the transient knockdown RSc cells 24 hrs after inoculation of HCV-JFH1 at an MOI of 2 was determined by a focus-forming assay at 48 hrs post-infection. Experiments were done in triplicate and each virus titer was calculated relative to the level in RSc cells transfected with a control siRNA (Con) which was assigned as 100%. (E) Intracellular HCV infectivity was determined by a focus-forming assay at 48 hrs post-inoculation of lysates by repeated freeze and thaw cycles as described in (D). (F) RSc cells were transiently transfected with a pool of control siRNA (Con) or a pool of siRNA specific for Alix, Vps4B, or CHMP4b (50 nM). At 24 hrs after the transfection, the cells were inoculated with HCV-JFH1 at an MOI of 0.2 and incubated for 48 hrs. Then, culture medium was changed and incubated for 24 hours. Western blotting of cell lysates 72 hrs post-infection with anti-β-actin, anti-HCV NS5A, or anti-HCV Core antibody is shown.
doi:10.1371/journal.pone.0014517.g002

Finally, we examined the subcellular localization of HCV Core and Brox, a novel farnesylated Bro1 domain-containing protein, since Brox was recently identified as a CHMP4-binding protein [27]. In this context, the Core partially colocalized with GFP-Brox in 293FT cells coexpressing of HCV Core and GFP-Brox (Fig. 5B). Importantly, we observed similar partial colocalization in HCV-JFH1-infected RSc cells expressing GFP-Brox (Fig. 5C). On the other hand, the CHMP4b-GFP alone was diffused in the cytoplasm of uninfected RSc cells (Fig. 5C). To examine the potential role of Brox in HCV life cycle, we established the Brox knockdown RSc cells by lentiviral vector expressing shRNA targeted to Brox (Fig. 5D). Consequently, we found that the release of HCV Core or the infectivity of HCV into the culture supernatants was significantly suppressed in the Brox knockdown cells 4 days after HCV-JFH1 infection (Fig. 5E and 5F), while the RNA replication of HCV-JFH1 was marginally affected in the knockdown cells (Fig. 5G) in spite of the very effective knockdown of Brox mRNA (Fig. 5D), suggesting that Brox is also required for the infectious HCV production.

Discussion

In this study, we have demonstrated that the ESCRT system is required for infectious HCV production, and that HCV Core but not NS5A binds to CHMP4b, a component of ESCRT-III. Although RNA replication of HCV-JFH1 was not affected in the TSG101 knockdown or the Alix knockdown cells, the infectivity of HCV in the culture supernatants was significantly suppressed in these knockdown cells after HCV-JFH1 infection (Fig. 1G and 1H). Furthermore, siRNA targeted to TSG101, Alix, Vps4B, or CHMP4b significantly suppressed HCV Core level or the infectivity of HCV in the culture supernatants (Fig. 1L, 1M, and

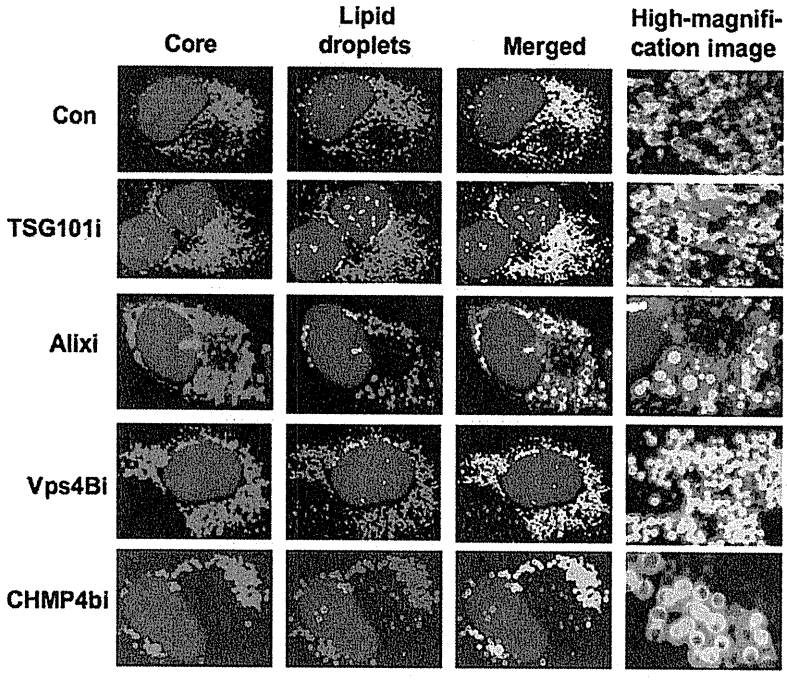

Figure 3. HCV Core is targeted to lipid droplets even in the ESCRT knockdown cells. The RSc cells transduced with a control lentiviral vector (Con), the TSG101 knockdown (TSG101i), the Alix knockdown (Alixi), the Vps4B knockdown (Vps4Bi), or the CHMP4b knockdown (CHMP4bi) cells were infected with HCV-JFH1. Cells were fixed 60 hrs post-infection and were then examined by confocal laser scanning microscopy. Cells were stained with anti-HCV Core (CP-9 and CP-11 mixture) and were then visualized with Cy3 (red). Lipid droplets and nuclei were stained with BODIPY 493/503 (green) and DAPI (blue), respectively. Images were visualized using confocal laser scanning microscopy. Colocalization is shown in yellow (Merged).
doi:10.1371/journal.pone.0014517.g003

2D), while the siRNA did not affect intracellular HCV Core level (Fig. 2E and 2F). Accordingly, we noticed some discrepancy that shRNA targeted to Vps4B or CHMP4b somewhat decreased intracellular HCV RNA replication (Fig. 1I), whereas siRNA targeted to TASG101, Alix, Vps4B or CHMP4b did not affect the RNA replication of subgenomic replicon of JFH1 (Fig. 2A and 2B). Furthermore, siRNAs targeted to TSG101, Alix, Vps4B, or CHMP4b did not affect HCV-O (genotype 1b) RNA replication using the OR6 assay system [17,18] (Fig. 2C), indicating that the ESCRT system is unrelated to the HCV RNA replication of genotype 1b. Thus, we suggested that the ESCRT system is not significant for HCV RNA replication. Within the family *Flaviviridae*, NS3 of the Japanese encephalitis virus (JEV) is also known to interact with TSG101 and microtubules, suggesting their potential roles in JEV assembly [28]. Accordingly, HCV NS3 has been involved in HCV particle assembly and infectivity [29,30]. However, whether HCV NS3 or another HCV protein binds to TSG101 remains to be investigated. At least, we did not observe the interaction between HCV NS5A and CHMP4b (Fig. 4D), Alix (Fig. 4D), TSG101, or Vps4B (data not shown).

Efficient enveloped virus release requires *cis*-acting viral late domains (L-domains), including P(T/S)AP, YPXnL (where X is any amino acid), and PPXY amino acid L-domain motif that are found in the structural proteins of other enveloped viruses [10,11]. Unlike the case with these enveloped viruses, we failed to find the three types of conserved viral L-domain motif in the HCV-JFH1 Core (data not shown). Nevertheless, we observed that the Core bound to CHMP4b, whereas NS5A did not (Fig. 4D), suggesting that the Core has a novel motif required for the HCV production. In this regard, Blanchard *et al.* reported that the aspartic acid at position 111 in the Core is crucial for virus assembly [31]. Interestingly, the conversion of the aspartic acid into alanine at amino acid 111 (PTDP to PTAP), which creates the PTAP L-domain motif, enhanced the release of HCV Core in the cell culture medium (a 2.5-fold increase) compared with the wild-type Core [31]. In contrast, Klein *et al.* demonstrated that the D111A mutation in the Core had no effect on HCV capsid assembly [32]. Furthermore, Murray *et al* found that serine 99, a putative phosphorylation site, in the Core was essential for infectious virion production [7]. In any event, the Core motif that is needed for interaction with the ESCRT components remains to be identified.

Ubiquitin modification of viral protein has been implicated in virion egress as well as in protein turnover. Indeed, the ubiquitin/proteasome system is required for the retrovirus budding machinery, since proteasome inhibition interferes with retroviral Gag polyprotein processing, release, and maturation. The ubiquitin modification of the HIV-1 p6 domain of Gag enhances TSG101 binding [12]. In the case of HCV Core, proteasomal degradation of the Core is mediated by two distinct mechanisms [33–36]. E6AP E3 ubiquitin ligase mediates ubiquitylation and degradation of the Core [34]. In contrast, proteasome activator PA28γ (11S regulator γ), an HCV Core-binding protein, is involved in the ubiquitin-independent degradation of the Core and HCV propagation [33,35,36]. However, little is known whether or not the ubiquitin modification of the Core might be involved in HCV egress like other enveloped viruses.

Finally, the identification of the site of viral particle assembly and budding is an intriguing issue. In case of HCV, at present, it is very difficult to visualize the HCV budding site in the infected cells by an electron microscopy. However, recent studies suggested that lipid droplets are an important cytoplasmic organelle for HCV production [4]. In this regard, Shavinskaya *et al.* demonstrated that

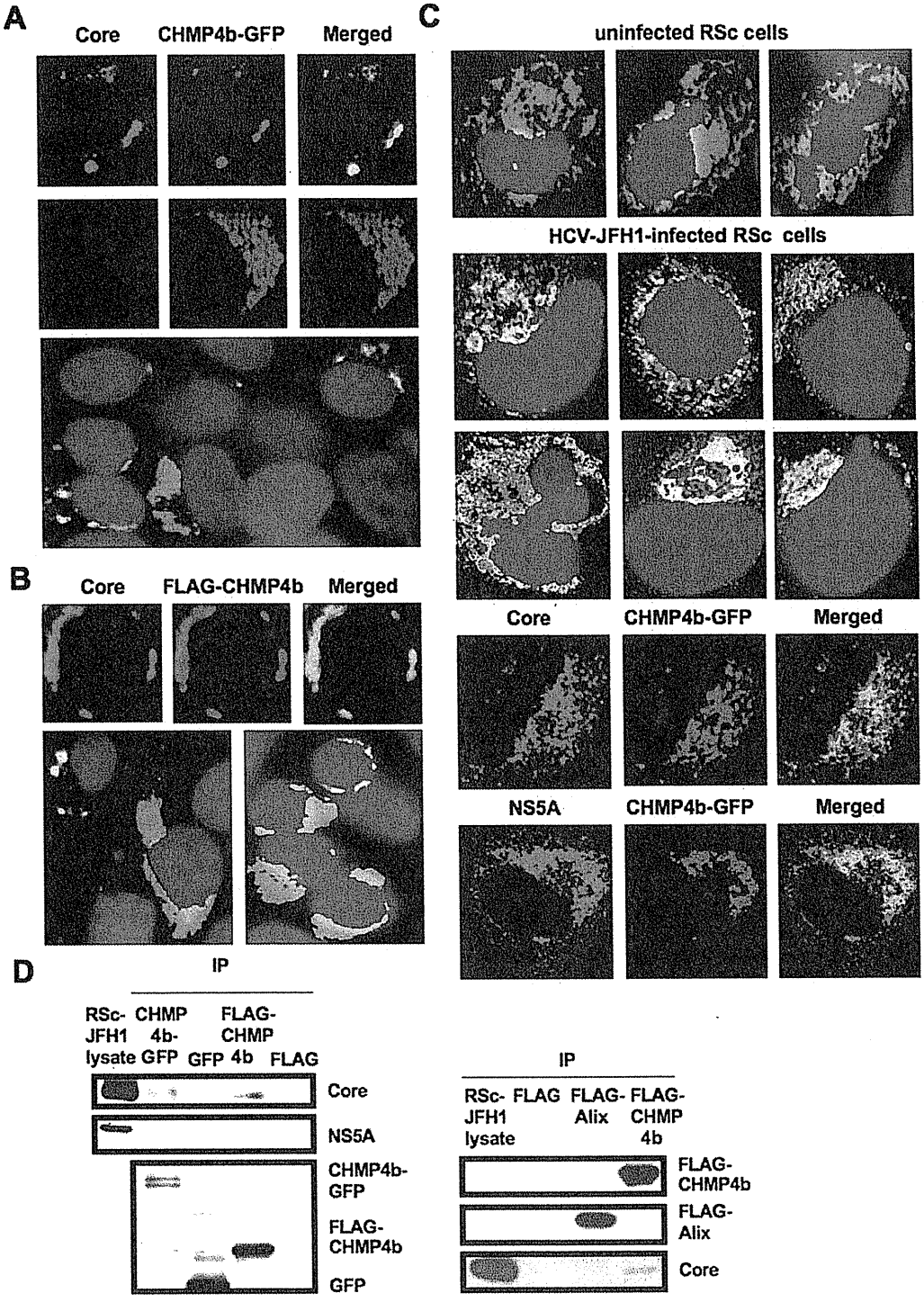

Figure 4. HCV Core interacts with CHMP4b. (A–C) HCV Core colocalizes with CHMP4b. 293FT cells cotransfected with 100 ng of pcDNA3/core (JFH1) and either 100 ng of pCHMP4b-GFP [39] (A) or pFLAG-CHMP4b [39] (B) were examined by confocal laser scanning microscopy. Cells were stained with anti-HCV Core and anti-FLAG polyclonal antibody and were then visualized with FITC (FLAG-CHMP4b) or Cy3 (Core). Images were visualized using confocal laser scanning microscopy. The right panels exhibit the two-color overlay images (Merged). Colocalization is shown in yellow. (C) The Core or NS5A partially colocalizes with CHMP4b in HCV-JFH1-infected RSc cells. RSc cells transfected with 100 ng of pCHMP4b-GFP were infected with HCV-JFH1. Cells were fixed 60 hrs post-infection and were then examined by confocal laser scanning microscopy as shown in panel (A). (D) HCV Core binds to CHMP4b. 293FT cells transfected with 4 μg of pCHMP4b-GFP, pEGFP C3 (Clontech), pcDNA3-FLAG, pcDNA3-FLAG-Alix or pFLAG-CHMP4b and RSc cells 5 days after inoculation of HCV-JFH1 at an MOI of 4 were lysed. The mixtures of these lysates were immunoprecipitated with either anti-FLAG or Living Colors A.v. monoclonal antibody (anti-GFP antibody), followed by immunoblot analysis using anti-HCV Core, anti-HCV NS5A, anti-FLAG, and/or Living Colors A.v. monoclonal antibody.
doi:10.1371/journal.pone.0014517.g004

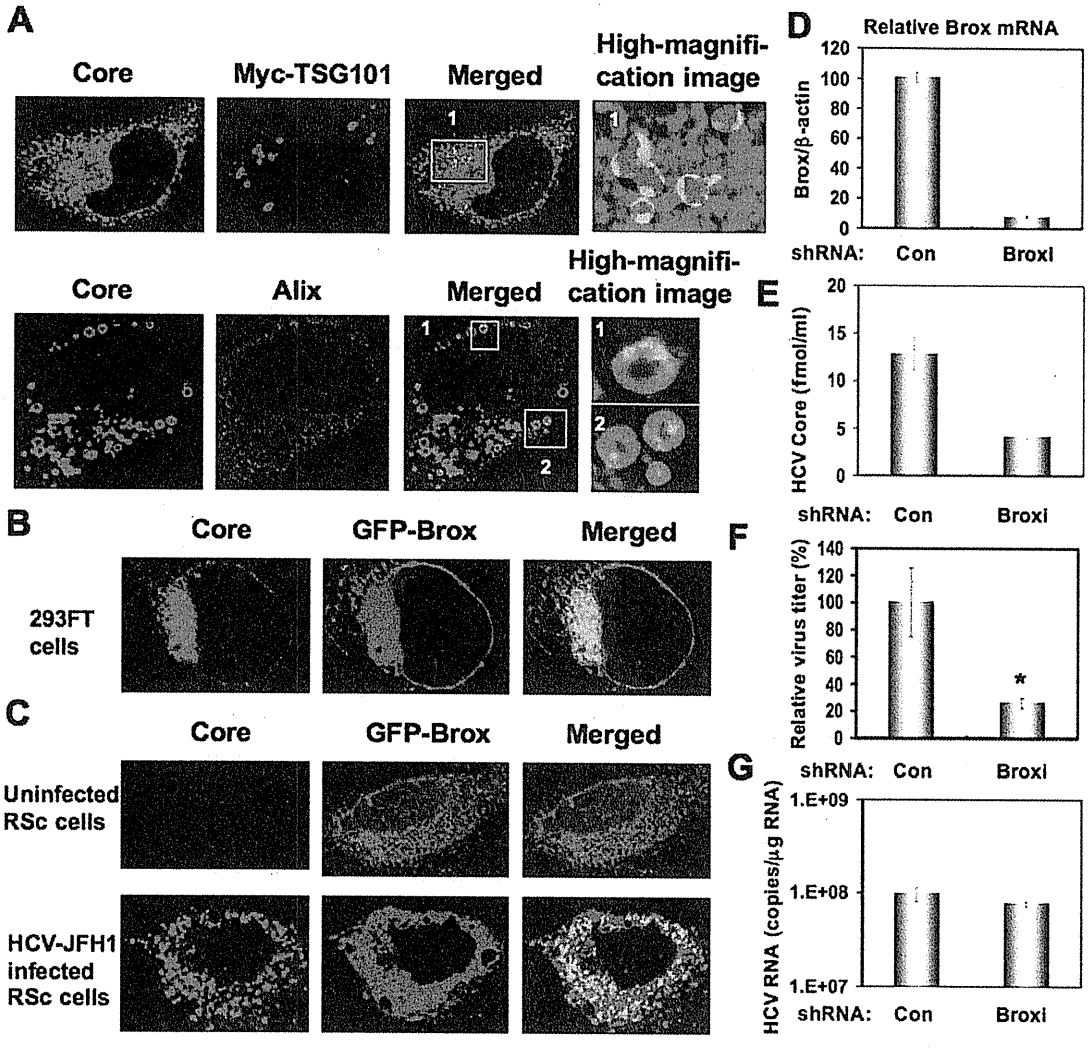

Figure 5. Brox is required for HCV life cycle. (A) Subcellular localization of Myc-tagged TSG101 in HCV-JFH1-infected RSc cells. RSc cells transfected with 100 ng of pBj-Myc-TSG101 [40] were infected with HCV-JFH1. Cells were fixed 60 hrs post-infection and were then examined by confocal laser scanning microscopy as shown in Fig. 3. High magnification image of area 1 is shown. Subcellular localization of endogenous Alix in HCV-JFH1-infected RSc cells 60 hrs post-infection. Cells were stained with anti-Alix and anti-HCV Core antibodies and were examined by confocal laser scanning microscopy. High magnification images of area 1 and area 2 are shown. (B) HCV Core partially colocalizes with Brox. 293FT cells cotransfected with 100 ng of pcDNA3/core (JFH1) and 100 ng of pmGFP-Brox^{WT} [27] were examined by confocal laser scanning microscopy. (C) The HCV Core partially colocalizes with Brox in HCV-JFH1-infected RSc cells. RSc cells transfected with 100 ng of pmGFP-Brox^{WT} were infected with HCV-JFH1. Cells were fixed 60 hrs post-infection and were then examined by confocal laser scanning microscopy. (D) Inhibition of Brox mRNA expression by the shRNA-producing lentiviral vector. Real-time LightCycler RT-PCR for Brox was performed as well as for β-actin mRNA in triplicate. Each mRNA level was calculated relative to the level in RSc cells transduced with a control lentiviral vector (Con) which was assigned as 100%. (E) The levels of HCV Core in the culture supernatants from the Brox knockdown RSc cells (Broxi) 72 hrs after inoculation of HCV-JFH1 were determined by ELISA. (F) The infectivity of HCV in the culture supernatants was determined by a focus-forming assay at 48 hrs post-infection. Experiments were done in triplicate and each virus titer was calculated relative to the level in RSc cells transduced with a control lentiviral vector (Con) which was assigned as 100%. Asterisks indicate significant differences compared to the control treatment. *$P<0.05$; **$P<0.01$. (G) The levels of intracellular genome-length HCV-JFH1 RNA in the cells used in (E) were monitored by real-time LightCycler RT-PCR.
doi:10.1371/journal.pone.0014517.g005

the lipid droplet-binding domain of the Core is a major determinant for efficient virus assembly [6]. The HCV Core induces lipid droplet redistribution in a microtubule- and dynein-dependent manner, since disrupting the microtubule network reduced the HCV titer, implicating transport networks in virus assembly and release [2]. Furthermore, Sandrin *et al.* reported that HCV envelope proteins localized to ESCRT-associated multivesicular body (MVB) [37]. Quite recently, Corless *et al.* have demonstrated that Vps4B and the ESCRT-III complex are required for HCV production [38]. Consistent with our findings, their dominant-negative forms of Vps4B and CHMP4B clearly suppressed HCV production. However, their dominant-negative forms of TSG101 and Alix failed to suppress the HCV production and they suggested that both TSG101 and Alix are unrelated to the HCV production. In contrast, we have demonstrated both TSG101 and Alix are also required for the infectious HCV

production by using shRNAs and siRNAs (Fig. 1). We may partly explain such discrepancy due to the difference of the methodology in our study utilized shRNAs and siRNAs instead of dominant-negative forms of TSG101 and Alix. Importantly, they demonstrated that the dominant-negative forms of Vps4B and CHMP4b did not affect the HCV RNA replication and the accumulation of intracellular infectious particles, suggesting that Vps4B and CHMP4b are unrelated to HCV RNA replication. Indeed, we have demonstrated that the ESCRT system is not required for the assembly of intracellular infectious HCV particles (Fig. 2E). Notably, we have demonstrated for the first time that HCV Core associated with CHMP4b (Fig. 4). Accordingly, we have also demonstrated that Brox, a CHMP4b binding protein, is required for HCV production (Fig. 5D–G). Taking together the past and present findings, we propose that the ESCRT system is involved in infectious HCV production after the HCV assembly that occurs on lipid droplets.

Acknowledgments

We thank D. Trono, R. Iggo, R. Agami, A. Takamizawa, and K. Shimotohno for pCMVΔR8.91, pMDG2, pSUPER, pRDI292, and anti-NS5A antibody, respectively. We also thank K. Abe for construction of pJRN/3-5B and T. Nakamura for his technical assistance.

Author Contributions

Conceived and designed the experiments: YA NK. Performed the experiments: YA MK. Analyzed the data: YA. Contributed reagents/materials/analysis tools: MM MI HD TW. Wrote the paper: YA NK.

References

1. Kato N, Hijikata M, Ootsuyama Y, Nakagawa M, Ohkoshi S, et al. (1990) Molecular cloning of the human hepatitis C virus genome from Japanese patients with non-A, non-B hepatitis. Proc Natl Acad Sci USA 87: 9524–9528.
2. Boulant S, Douglas MW, Moody L, Budkowska A, Targett-Adams P, et al. (2008) Hepatitis C virus core protein induces lipid droplet redistribution in a microtubule- and dynein-dependent manner. Traffic 9: 1268–1282.
3. Masaki T, Suzuki R, Murakami K, Aizaki H, Ishii K, et al. (2008) Interaction of hepatitis C virus nonstructural protein 5A with core protein is critical for the production of infectious virus particles. J Virol 82: 7964–7976.
4. Miyanari Y, Atsuzawa K, Usuda N, Watashi K, Hishiki T, et al. (2007) The lipid droplet is an important organelle for hepatitis C virus production. Nat Cell Biol 9: 1089–1097.
5. Shi ST, Polyak SJ, Tu H, Taylor DR, Gretch DR, et al. (2002) Hepatitis C virus NS5A colocalizes with the core protein on lipid droplets and interacts with apolipoproteins. Virology 292: 198–210.
6. Shavinskaya A, Boulant S, Penin F, McLauchlan J, Bartenschlager R (2007) The lipid droplet binding domain of hepatitis C virus core protein is a major determinant for efficient virus assembly. J Biol Chem 282: 37158–37169.
7. Murray CL, Jones CT, Tassello J, Rice CM (2007) Alanine scanning of the hepatitis C virus core protein reveals numerous residues essential for production of infectious virus. J Virol 81: 10220–10231.
8. Appel N, Zayas M, Miller S, Krijnse-Locker J, Schaller T, et al. (2008) Essential role of domain III of nonstructural protein 5A for hepatitis C virus infectious particle assembly. PLOS Pathog 4: e1000035.
9. Tellinghuisen TL, Foss KL, Treadaway J (2008) Regulation of hepatitis C virion production via phosphorylation of the NS5A protein. PLoS Pathog 4: e1000032.
10. Bieniasz PD (2006) Late budding domains and host proteins in enveloped virus release. Virology 344: 55–63.
11. Chen BJ, Lamb RA (2008) Mechanisms for enveloped virus budding: Can some viruses do without an ESCRT? Virology 372: 221–232.
12. Garrus JE, von Schwedler UK, Pornillos OW, Morham SG, Zavitz KH, et al. (2001) Tsg101 and vacuolar protein sorting pathway are essential for HIV-1 budding. Cell 107: 55–65.
13. Wakita T, Pietschmann T, Kato T, Date T, Miyamoto M, et al. (2005) Production of infectious hepatitis C virus in tissue culture from a cloned viral genome. Nat Med 11: 791–796.
14. Ariumi Y, Kuroki M, Abe K, Dansako H, Ikeda M, et al. (2007) DDX3 DEAD-box RNA helicase is required for hepatitis C virus RNA replication. J Virol 81: 13922–13926.
15. Ariumi Y, Kuroki M, Dansako H, Abe K, Ikeda M, et al. (2008) The DNA damage sensors, ataxia-telangiectasia mutated kinase and checkpoint kinase 2 are required for hepatitis C virus RNA replication. J Virol 82: 9639–9646.
16. Kuroki M, Ariumi Y, Ikeda M, Dansako H, Wakita T, et al. (2009) Arsenic trioxide inhibits hepatitis C virus RNA replication through modulation of the glutathione redox system and oxidative stress. J Virol 83: 2338–2348.
17. Ikeda M, Abe K, Dansako H, Nakamura T, Naka K, et al. (2005) Efficient replication of a full-length hepatitis C virus genome, strain O, in cell culture, and development of a luciferase reporter system. Biochem Biophys Res Commun 329: 1350–1359.
18. Ikeda M, Abe K, Yamada M, Dansako H, Naka K, et al. (2006) Different anti-HCV profiles of statins and their potential combination therapy with interferon. Hepatology 44: 117–125.
19. Ariumi Y, Kaida A, Hatanaka M, Shimotohno K (2001) Functional cross-talk of HIV-1 Tat with p53 through its C-terminal domain. Biochem Biophys Res Commun 287: 556–561.
20. Abe K, Ikeda M, Ariumi Y, Dansako H, Wakita T, et al. (2009) HCV genotype 1b chimeric replicon with NS5B of JFH-1 exhibited resistance to cyclosporine A. Arch Virol 154: 1671–1677.
21. Ariumi Y, Ego T, Kaida A, Matsumoto M, Pandolfi PP, et al. (2003) Distinct nuclear body components, PML and SMRT, regulate the trans-acting function of HTLV-1 Tax oncoprotein. Oncogene 22: 1611–1619.
22. Brummelkamp TR, Bernard R, Agami R (2002) A system for stable expression of short interfering RNAs in mammalian cells. Science 296: 550–553.
23. Bridge AJ, Pebernard S, Ducraux A, Nicoulaz AL, Iggo R (2003) Induction of an interferon response by RNAi vectors in mammalian cells. Nat Genet 34: 263–264.
24. Ariumi Y, Priscilla T, Masutani M, Trono D (2005) DNA damage sensors ATM, ATR, DNA-PKcs, and PARP-1 are dispensable for human immunodeficiency virus type 1 integration. J Virol 79: 2973–2978.
25. Naldini L, Blömer U, Gallay P, Ory D, Mulligan R, et al. (1996) In vivo gene delivery and stable transduction of non-dividing cells by a lentiviral vector. Science 272: 263–267.
26. Zufferey R, Nagy D, Mandel RJ, Naldini L, Trono D (1997) Multiply attenuated lentiviral vector achieves efficient gene delivery in vivo. Nat Biotechnol 15: 871–875.
27. Ichioka F, Kobayashi R, Katoh K, Shibata H, Maki M (2008) Brox, a novel farnesylated Brol domain-containing protein that associates with charged multivesicular body protein 4 (CHMP4). FEBS J 275: 682–692.
28. Chiou CT, Hu CCA, Chen PH, Liao CL, Lin YL, et al. (2003) Association of Japanese encephalitis virus NS3 protein with microtubules and tumor susceptibility gene 101 (TSG101) protein. J Gen Virol 84: 2795–2805.
29. Yi M, Ma Y, Yates J, Lemon SM (2007) Compensatory mutations in E1, p7, NS2, and NS3 enhance yields of cell culture-infectious intergenotypic chimeric hepatitis C virus. J Virol 81: 629–638.
30. Ma Y, Yates J, Liang Y, Lemon SM, Yi M (2008) NS3 helicase domains involved in infectious intracellular hepatitis C virus particle assembly. J Virol 82: 7624–7639.
31. Blanchard E, Hourioux C, Brand D, Ait-Goughoulte M, Moreau A, et al. (2003) Hepatitis C virus-like particle budding: Role of the core protein and importance of its Asp^{111}. J Virol 77: 10131–10138.
32. Klein KC, Dellos SR, Lingappa JR (2005) Identification of residues in hepatitis C virus core protein that are critical for capsid assembly in a cell-free system. J Virol 79: 6814–6826.
33. Moriishi K, Okabayashi T, Nakai K, Moriya K, Koike K, et al. (2003) Proteasome activator 28γ-dependent nuclear retention and degradation of hepatitis C virus core protein. J Virol 77: 10237–10249.
34. Shirakawa M, Murakami K, Ichimura T, Suzuki R, Shimoji T, et al. (2007) E6AP ubiquitin ligase mediates ubiquitylation and degradation of hepatitis C virus core protein. J Virol 81: 1174–1185.
35. Suzuki R, Moriishi K, Fukuda K, Shirakura M, Ishii K, et al. (2009) Proteasomal turnover of hepatitis C virus core protein is regulated by two distinct mechanisms: a ubiquitin-dependent mechanism and a ubiquitin-independent but PA28γ-dependent mechanism. J Virol 83: 2389–2392.
36. Moriishi K, Shoji I, Mori R, Suzuki R, Suzuki T, et al. (2010) Involvement of PA28gamma in the propagation of hepatitis C virus. Hepatology 52: 411–420.
37. Sandrin V, Boulanger P, Penin F, Granier C, Cosset FL, et al. (2005) Assembly of functional hepatitis C virus glycoproteins on infectious pseudoparticles occurs intracellularly and requires concomitant incorporation of E1 and E2 glycoproteins. J Gen Virol 86: 3189–3199.
38. Corless L, Crump CM, Griffin SD, Harris M (2010) Vps4 and ESCRT-III complex are required for the release of infectious hepatitis C virus particles. J Gen Virol 91: 362–372.
39. Katoh K, Shibata H, Suzuki H, Nara A, Ishidoh K, et al. (2003) The ALG-2-interacting protein Alix associates with CHMP4b, a human homologue of yeast Snf7 that is involved in multivesicular body sorting. J Biol Chem 278: 39104–39113.
40. Katoh K, Suzuki H, Terasawa Y, Mizuno T, Yasuda J, et al. (2005) The penta-EF-hand protein ALG-2 interacts directly with the ESCRT-I component TSG101, and Ca^{2+}-dependently co-localizes to aberrant endosomes with dominant-negative AAA ATPase SKD1/Vps4B. Biochem J 391: 677–685.

Liver INTERNATIONAL
OFFICIAL JOURNAL OF THE INTERNATIONAL ASSOCIATION FOR THE STUDY OF THE LIVER

Liver International ISSN 1478-3223

BASIC STUDIES

Anti-ulcer agent teprenone inhibits hepatitis C virus replication: potential treatment for hepatitis C

Masanori Ikeda[1]*, Yoshinari Kawai[1,2]*, Kyoko Mori[1], Masahiko Yano[1,3], Ken-ichi Abe[1], Go Nishimura[1], Hiromichi Dansako[1], Yasuo Ariumi[1], Takaji Wakita[4], Kazuhide Yamamoto[2] and Nobuyuki Kato[1]

1 Department of Tumor Virology, Okayama University Graduate School of Medicine, Dentistry, and Pharmaceutical Sciences, Okayama, Japan
2 Department of Gastroenterology and Hepatology, Okayama University Graduate School of Medicine, Dentistry, and Pharmaceutical Sciences, Okayama, Japan
3 Division of Gastroenterology and Hepatology, Graduate School of Medical and Dental Sciences, Niigata University, Niigata City, Japan
4 Department of Virology II, National Institute of Infectious Diseases, Tokyo, Japan

Keywords
geranylgeranylation – HCV – Selbex – statin – teprenone

Correspondence
Masanori Ikeda, MD, PhD, Department of Tumor Virology, Okayama University Graduate School of Medicine, Dentistry, and Pharmaceutical Sciences, 2-5-1 Shikata-cho, Okayama 700-8558, Japan
Tel: +81-86-235-7386
Fax: +81-86-235-7392
e-mail: maikeda@md.okayama-u.ac.jp

Received 11 October 2010
Accepted 7 February 2011

DOI:10.1111/j.1478-3231.2011.02499.x

Abstract

Background: Previously we reported that 3-hydroxy-3-methylglutaryl coenzyme A reductase inhibitors, statins, inhibited hepatitis C virus (HCV) RNA replication. Furthermore, recent reports revealed that the statins are associated with a reduced risk of hepatocellular carcinoma and lower portal pressure in patients with cirrhosis. The statins exhibited anti-HCV activity by inhibiting geranylgeranylation of host proteins essential for HCV RNA replication. Geranylgeranyl pyrophosphate (GGPP) is a substrate for geranylgeranyltransferase. Therefore, we examined the potential of geranyl compounds with chemical structures similar to those of GGPP to inhibit HCV RNA replication. *Methods:* We tested geranyl compounds [geranylgeraniol, geranylgeranoic acid, vitamin K_2 and teprenone (Selbex)] for their effects on HCV RNA replication using genome-length HCV RNA-replicating cells (the OR6 assay system) and a JFH-1 infection cell culture system. Teprenone is the major component of the anti-ulcer agent, Selbex. We also examined the anti-HCV activities of the geranyl compounds in combination with interferon (IFN)-α or statins. *Results:* Among the geranyl compounds tested, only teprenone exhibited anti-HCV activity at a clinically achievable concentration. However, other anti-ulcer agents tested had no inhibitory effect on HCV RNA replication. The combination of teprenone and IFN-α exhibited a strong inhibitory effect on HCV RNA replication. Although teprenone alone did not inhibit geranylgeranylation, surprisingly, statins' inhibitory action against geranylgeranylation was enhanced by cotreatment with teprenone. *Conclusions:* The anti-ulcer agent teprenone inhibited HCV RNA replication and enhanced statins' inhibitory action against geranylgeranylation. This newly discovered function of teprenone may improve the treatment of HCV-associated liver diseases as an adjuvant to statins.

Hepatitis C virus (HCV) infection frequently causes persistent hepatitis and leads to cirrhosis and hepatocellular carcinoma (HCC). Currently, the combination therapy of pegylated interferon (IFN) with ribavirin is available for patients with chronic hepatitis C (CH C) and yields a sustained virological response rate of about 50% (1). However, about half of CH C patients are still susceptible to the progression of the disease to fatal cirrhosis and HCC. Therefore, the development of more effective reagents for the treatment of HCV infection is urgent.

To overcome this problem, we developed a genome-length HCV RNA (strain O of genotype 1b) replication system (OR6) with luciferase as a reporter, which facilitated the prompt and precise monitoring of HCV RNA replication in hepatoma cells (HuH-7-derived OR6 cells) (2). Using this OR6 system, we recently reported that 3-hydroxy-3-methylglutaryl coenzyme A (HMG-CoA) reductase inhibitors, statins, inhibited HCV RNA replication efficiently (3–5). Among five statins – fluvastatin (FLV), atorvastatin (ATV), simvastatin (SIV), pravastatin (PRV) and lovastatin (LOV) – FLV exhibited the strongest anti-HCV activity, while PRV had no effect on HCV RNA replication (3, 6). More recently, Bader *et al.* (7) demonstrated that FLV inhibited HCV RNA replication

*Contributed equally.

in humans. Furthermore, recent reports revealed that the statins were associated with a reduced risk of HCC (8) and lower portal pressure in patients with cirrhosis (9).

Statins targeted the mevalonate pathway. This pathway is branched after farnesyl pyrophosphate (FPP) into cholesterol and geranylgeranyl pyrophosphate (GGPP) biosynthesis pathways. The inhibition of GGPP but not of cholesterol is essential for HCV RNA replication in the inhibitory activity of statins (3, 10, 11). To date, one of the proteins, FBL2, was reported as the host protein essential for HCV RNA replication. HCV RNA replication requires geranylgeranylation of FBL2 by geranylgeranyltransferase with GGPP (12).

We have attempted to examine the effects of geranyl compounds [geranylgeraniol (GGOH), geranylgeranoic acid, vitamin K_2 (VK2) and teprenone] on HCV RNA replication using the OR6 assay system and the JFH-1 infection cell culture system, because their chemical formulas are similar to that of the GGPP, a substrate for geranylgeranyltransferase in geranylgeranylation (13–15). The anti-ulcer agent teprenone (also called geranylgeranylacetone) is reported to block the function of GGPP by the competitive inhibition of the mevalonate pathway (16). Teprenone is the major component of the clinically used anti-ulcer reagent, Selbex.

Here, we reported the inhibitory activity of teprenone on HCV RNA replication and the effect of teprenone in combination with statins on their inhibitory action against geranylgeranylation.

Materials and methods

Reagents and antibodies

Teprenone (Selbex), geranylgeranoic acid, ecabet sodium and sofalcon, gefarnate were purchased from Eisai Co. Ltd (Tokyo, Japan), BIOMOL (Plymouth Meeting, PA, USA), Mitsubishi Tanabe Pharma (Osaka, Japan), Taisho Pharmaceutical Co. (Tokyo, Japan) and Dainippon Sumitomo Pharma Co. Ltd (Osaka, Japan) respectively. GGPP, GGOH, VK2, IFN-α, vitamin E, linoleic acid and mevalonate were purchased from Sigma (St Louis, MO, USA). Cyclosporine A, FLV, LOV and PRV were purchased from Calbiochem (Los Angeles, CA, USA). ATV, SIV and pitavastatin (PTV) were purchased from Astellas Pharma Inc. (Tokyo, Japan), Banyu Pharmaceutical Co. Ltd (Tokyo, Japan), and Kowa Co. Ltd (Nagoya, Japan) respectively.

The antibodies used in this study were those specific to the Core (CP11, Institute of Immunology, Tokyo), NS5A (a generous gift from Dr A. Takamizawa, Research Foundation for Microbial Diseases, Osaka University), NS5B (a generous gift from Dr M. Kohara, Tokyo Metropolitan Institute of Medical Science) and β-actin (Sigma). Anti-heat shock protein (HSP) 90 and anti-HSP70 antibodies were purchased from BD Bioscience (San Jose, CA, USA). Anti-Rap1A (sc-1482) and anti-Rap1 (sc-65) antibodies were purchased from Santa Cruz Biotechnology (Santa Cruz, CA, USA).

Cell cultures

OR6 is a cell line cloned from ORN/C-5B/KE RNA-replicating HuH-7 cells as described previously (2) and cultured in Dulbecco's modified Eagle's medium supplemented with 10% fetal bovine serum, penicillin, streptomycin and G418 (300 μg/ml; Geneticin, Invitrogen, Carlsbad, CA, USA). ORN/C-5B/KE RNA is derived from HCV-O, and OR6c cells are cured OR6 cells from which HCV RNA was eliminated by IFN-α treatment as described previously (2). HCV-O/RLGE is the authentic HCV RNA containing adaptive mutations of Q1112R, P1115L, E1203G and K1609E in the NS3 region and replicates efficiently in OR6c cells.

OR6 reporter assay

For the *Renilla* luciferase (RL) assay, $1.0–1.5 \times 10^4$ OR6 cells were plated onto 24-well plates in triplicate and precultured for 24 h. The cells were treated with each compound for 72 h. Then, the cells were harvested and subjected to an RL assay according to the manufacturer's protocol (2).

Western blot analysis

For western blot analysis, $4–4.5 \times 10^4$ OR6 or OR6c cells harbouring HCV-O/RLGE RNA were plated onto six-well plates and cultured for 24 h, and were then treated with each compound for 72 h. Preparation of the cell lysates, sodium dodecyl sulphate-polyacrylamide gel electrophoresis and immunoblotting were then performed as described previously (17).

Cell growth assay

To examine the effect of each reagent on OR6 cell growth, $6.0–6.5 \times 10^4$ OR6 cells were plated onto six-well plates in triplicate and were precultured for 24 h. The cells were treated with or without each compound for 72 h, and then the viable cells were counted after trypan blue dye treatment as described previously (18).

WST-1 cell proliferation assay

The OR6 cells (2×10^3 cells) were plated onto a 96-well plate in triplicate at 24 h before treatment with each reagent. The cells at 24, 48 and 72 h after treatment were subjected to a WST-1 cell proliferation assay (Takara Bio, Otsu, Japan) according to the manufacturer's protocol.

Reverse transcription-polymerase chain reaction

Reverse transcription-polymerase chain reaction (RT-PCR) for HMG-CoA reductase and for glyceraldehyde-3-phosphate dehydrogenase (GAPDH) was performed by a method described previously (19). Briefly, using cellular total RNAs (2 μg), cDNA was synthesized using Superscript II with the oligo dT primer. One-tenth of the synthesized cDNA was subjected to PCR with the

following primer pairs: HMG-CoA reductase, 5′-ATGCC ATCCCTGTTGGAGTG-3′ and 5′-TGTTCATCCCCATG GCATCCC-3′; and GAPDH, 5′-GACTCATGACCACAG TCCATGC-3′ and 5′-GAGGAGACCACCTGGTGCTCA G-3′.

Hepatitis C virus infection experiment

For the infection experiment with the JFH-1 virus, HuH-7-derived RSc cells (1×10^5 cells) were plated onto six-well plates and cultured for 24 h (20). Then, the cells were infected with 100 µl (equivalent to a multiple of infection of 0.1–0.2) of inoculum and cultured for 24 h. The cells were treated with each reagent for 72 h. The culture supernatants and cells were collected for quantification of the Core by an enzyme-linked immunosorbent assay (ELISA) (Mitsubishi Kagaku Bio-Clinical Laboratories, Tokyo, Japan) and for western blot analysis respectively.

Statistical analysis

The luciferase activities were statistically compared between the various treatment groups using Student's *t*-test. *P* values of < 0.05 were considered statistically significant. The mean ± standard deviation is determined from at least three independent experiments.

Results

Anti-hepatitis C virus activity of teprenone is a unique feature not only among geranyl compounds but also among anti-ulcer agents

The mevalonate pathway is divided into two branches: cholesterol synthesis and GGPP synthesis pathways (Fig. 1). The statins exhibited anti-HCV activity via inhibition of geranylgeranylation of host proteins essential for HCV RNA replication. Therefore, we examined the effects of geranyl compounds [GGOH, geranylgeranoic acid, VK2 and teprenone (Selbex)] on HCV RNA replication using the OR6 assay system, because their chemical structures are similar to that of the GGPP (Fig. 2A) (16). Teprenone inhibited HCV RNA replication in a dose-dependent manner without affecting OR6 cell growth up to a concentration of 20 µg/ml (Fig. 2B). The 50% effective concentration (EC_{50}) of teprenone is 5.3 µg/ml. On the other hand, GGOH, geranylgeranoic acid and VK2 did not inhibit HCV RNA replication at the concentration without cytotoxicity (Fig. 2C–E). We also demonstrated that teprenone did not affect cell proliferation within this concentration (supporting information, Fig. S1A). These results suggest that anti-HCV activity of teprenone was not a common feature among geranyl compounds.

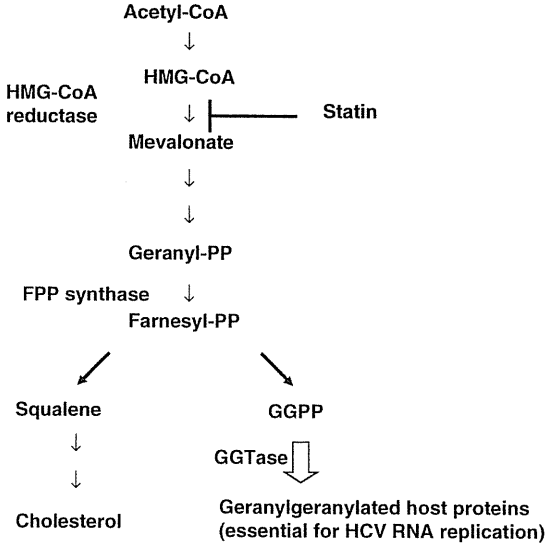

Fig. 1. Schema of the mevalonate pathway.

Teprenone is used for patients with gastritis and gastric ulcers. Therefore, we examined anti-ulcer agents for their inhibitory effects against HCV RNA replication. The chemical structures of three anti-ulcer agents – ecabet sodium, sofalcon and gefarnate – are shown in supporting information, Figure S1B. None of these agents exhibited inhibitory effects on HCV RNA replication (supporting information, Fig. S1C–E). These results indicate that the anti-HCV activity of teprenone may not be a common feature among anti-ulcer agents.

Teprenone inhibited authentic hepatitis C virus RNA replication

The genome-length HCV RNA replicating in the OR6 cells contained three non-natural elements – RL, neomycin phosphotransferase and encephalomyocarditis virus internal ribosomal entry site. To further confirm that the anti-HCV activity of teprenone was not because of the inhibition of these three exogenous genes or their products, we used authentic 9.6 kb HCV RNA-replicating cells. We introduced *in vitro* synthesized HCV-O/RLGE RNA into cured OR6c cells (Fig. 3A). As shown in Figure 3B, teprenone inhibited Core expression in HCV-O/RLGE-replicating OR6c cells in a dose-dependent manner. These results indicate that the anti-HCV activity of teprenone was because of the inhibition of HCV RNA itself, but not exogenous genes or their products.

Teprenone enhanced anti-hepatitis C virus activity of interferon-α

We examined whether or not teprenone would enhance the anti-HCV activity of IFN-α. We did this by studying the inhibitory effects of combinations of IFN-α (0, 2.5, 5 and 10 IU/ml) and teprenone (0, 10 and 20 µg/ml) using the OR6 assay system. Teprenone enhanced the anti-HCV activity of IFN-α in a dose-dependent manner (Fig. 4). Teprenone with IFN-α also inhibited Core expression (Fig. 4). We also demonstrated that teprenone did not

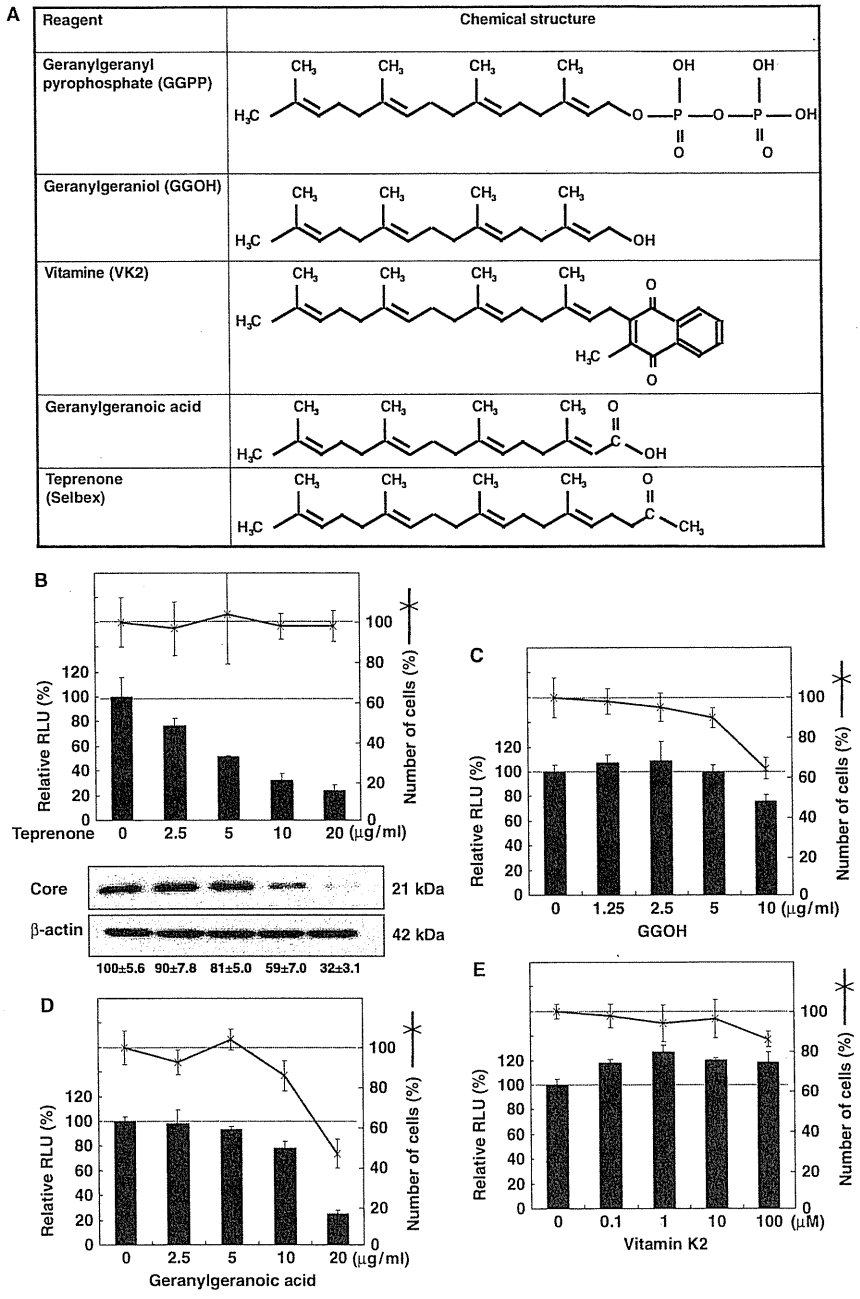

Fig. 2. The effects of geranyl compounds and anti-ulcer agents on hepatitis C virus (HCV) RNA replication. (A) Structures of geranyl compounds. (B) Anti-HCV activity of teprenone on HCV RNA replication in OR6 cells. OR6 cells were treated with teprenone (0, 2.5, 5, 10 and 20 μg/ml) for 72 h. *Renilla* luciferase (RL) activity for HCV RNA replication is shown as a percentage of control. Each bar represents the average with standard deviations of triplicate data points. Cell viability was also shown as a percentage of control. After 72-h treatment, the production of the Core was analysed by immunoblotting using anti-Core antibody (lower panel). β-actin was used as a control for the amount of protein loaded per lane. The signal intensities of Core from three independent assays were quantified by densitometry and normalized by that of β-actin. Each of the mean ± standard deviation is under the lower panel. (C to E) OR6 cells were treated with geranylgeraniol (0, 1.25, 2.5, 5 and 10 μg/ml) (C), geranylgeranoic acid (0, 2.5, 5, 10 and 20 μg/ml) (D) and VK2 (0, 0.1, 1, 10 and 100 μM) (E) for 72 h. RL activity and cell viability after treatment were determined as shown in (B).

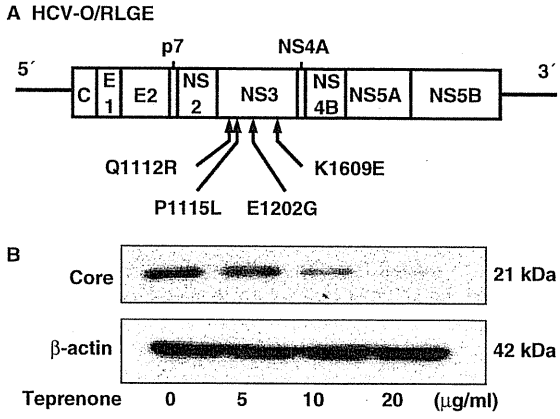

Fig. 3. Teprenone inhibited authentic hepatitis C virus (HCV) RNA replication. (A) Schematic gene organization of genome-length HCV-O/RLGE RNA. The positions of four adaptive mutations – Q1112R, P1115L, E1203G and K1609E – are indicated by arrows. (B) HCV-O/RLGE RNA was introduced into OR6c cells by electroporation as described previously (5). The cells were treated with teprenone (0, 5, 10 and 20 μg/ml) for 72 h and then the production of the Core was analysed by immunoblotting using anti-Core antibody.

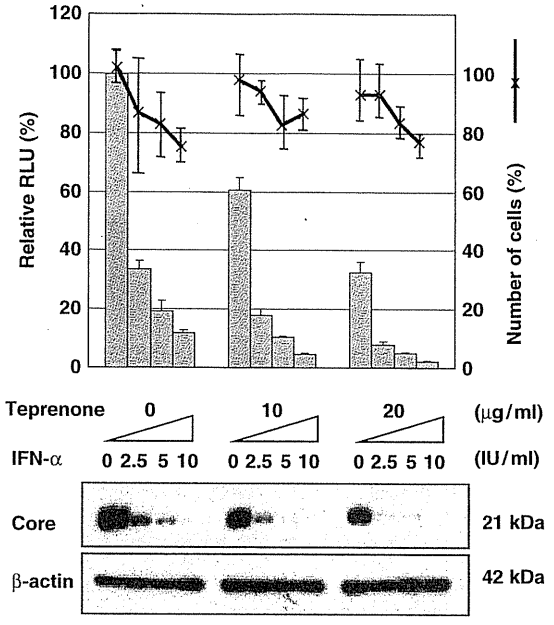

Fig. 4. Teprenone enhanced the anti-hepatitis C virus activity of interferon (IFN)-α. OR6 cells were cotreated with IFN-α (0, 2.5, 5 and 10 IU/ml) and teprenone (0, 10 and 20 μg/ml) for 72 h. *Renilla* luciferase assay was performed as described in Figure 2B. Production of the Core was analysed by immunoblotting using anti-Core antibody. The cells at 24, 48 and 72 h after treatment were subjected to a WST-1 cell proliferation assay.

affect cell proliferation within this concentration (Fig. 4). These results suggest that teprenone may be a new candidate as a complement to IFN therapy.

Teprenone exhibited anti-hepatitis C virus activity in the JFH-1 infection system

We examined the anti-HCV activity of teprenone in the JFH-1 infection system (13–15). We treated the cells with teprenone (0, 5, 10 and 20 μg/ml) at 24-h post-JFH-1 infection and cultured them for 72 h. The culture supernatants and cells were subjected to quantification of the Core by ELISA and western blot analysis respectively. Teprenone decreased the HCV Core in the supernatant (upper panel in Fig. 5A) and in the cells (lower panel in Fig. 5A) in a dose-dependent manner.

We next tested whether or not teprenone (0, 10 and 20 μg/ml) enhanced IFN-α's (0, 2.5 and 5 IU/ml) anti-HCV activity in the JFH-1 infection system. As shown in Figure 5B, teprenone enhanced the anti-HCV activity of IFN-α in a dose-dependent manner. These results suggest that teprenone also possessed anti-HCV activity in the JFH-1 infection system.

Teprenone did not inhibit geranylgeranylation

As shown in Figure 2A, the chemical structure of teprenone is similar to that of GGPP. Therefore, we examined the possibility that teprenone inhibits geranylgeranylation. Geranylgeranyl proteins possessed the C-A-A-X motif at the C-terminal of the protein: C is cystein; A is aliphatic amino acid; and X is typically leucine (or rarely isoleucine, valine or phenylalanine). Rap1A is one of the Ras-related proteins and selected to monitor the status of geranylgeranylation. We used anti-Rap1A antibody (sc-1482), which recognized only nongeranylgeranylated Rap1A (21, 22). Therefore, geranylgeranylated Rap1A is not recognized with this antibody. On the other hand, anti-Rap1 antibody (sc-65) recognizes Rap1A and Rap1B independent of the state of geranylgeranylation (22). In the following experiments, we used anti-Rap1A antibody (sc-1482) to monitor the state of geranylgeranylation.

OR6 cells were treated with PTV (1.25 μM) or teprenone (20 μg/ml) or neither. The cells were collected after treatment and subjected to luciferase assay and western blot analysis. In the untreated cells, nongeranylgeranylated Rap1A bands were not detected (Fig. 6A). PTV inhibited geranylgeranylation at 3 h and reached a plateau 12 h after treatment along with nongeranylgeranylated Rap1A bands (Fig. 6A). On the other hand, geranylgeranylation was not inhibited in the cells with teprenone treatment (Fig. 6A).

We then tested the effect of mevalonate cotreatment with PTV or teprenone. Mevalonate negated PTV's inhibitory action against geranylgeranylation and led to the loss of PTV's anti-HCV activity (Fig. 6B). However, mevalonate did not affect the anti-HCV activity of teprenone (Fig. 6B). These results indicate that teprenone

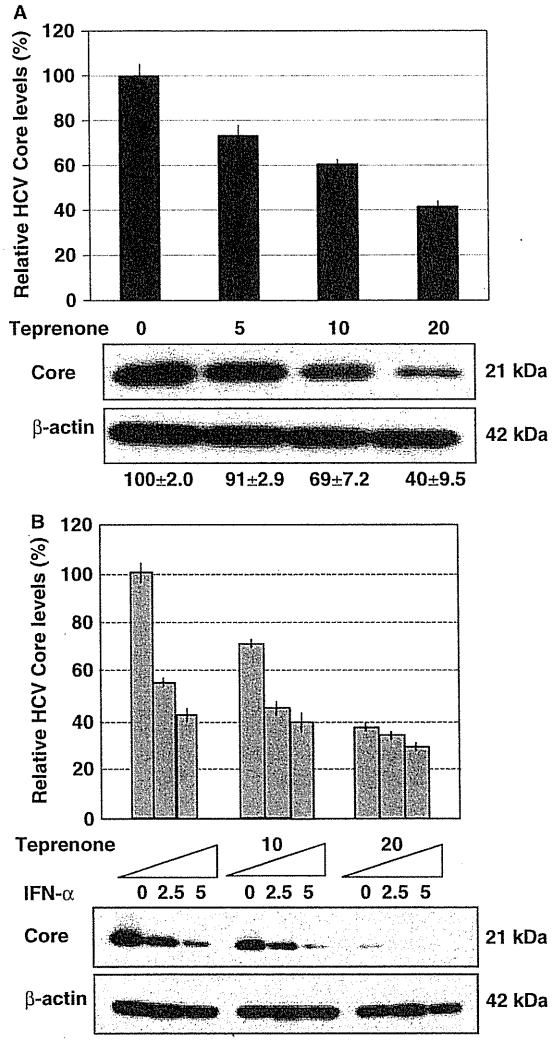

Fig. 5. Teprenone exhibited anti-hepatitis C virus (HCV) activity in the JFH-1 infection system. (A) Teprenone inhibited JFH-1 replication. HuH-7-derived RSc cells were infected with the JFH-1 virus for 24 h and were then treated with teprenone (0, 5, 10 and 20 μg/ml) for 72 h. The supernatant and the cells were subjected to quantification of the Core by ELISA and western blot analysis respectively. The signal intensities of Core were quantified by densitometry and the mean ± standard deviation is under the lower panel as shown in Figure 2B. (B) Teprenone enhanced interferon (IFN)-α's anti-HCV activity in the JFH-1 infection system. JFH-1 virus-infected cells were treated with teprenone (0, 10 and 20 μg/ml) and IFN-α (0, 2.5 and 5 IU/ml) for 72 h and then subjected to Core quantification by ELISA and western blot analysis as shown in (A).

inhibits HCV RNA replication without the inhibition of geranylgeranylation.

Statin's inhibition of HMG-CoA reductase decreased cholesterol synthesis and led to the increase of HMG-CoA reductase expression by positive feedback (3). The mRNA of HMG-CoA reductase was increased with PTV treatment but not with teprenone treatment (supporting information, Fig. S3A and B). This result suggests that teprenone, unlike PTV, did not lower the cholesterol synthesis.

The chemical structure of teprenone, which is the major component of Selbex, is similar to that of GGPP, a substrate for geranylgeranyltransferase. Therefore, we ruled out the possibility that teprenone was incorporated into host proteins instead of GGPP and led to the loss of function of the host proteins, when endogenous GGPP was depleted by PTV in OR6 cells. The nongeranylgeranylated Rap1A was detected when OR6 cells were treated with PTV (lane 3; Fig. 6C). However, exogenous GGPP decreased nongeranylgeranylated Rap1A in PTV-treated OR6 cells (lane 4; Fig. 6C). If teprenone was incorporated into Rap1A instead of GGPP and formed a psuedo-geranylgeranylation, Rap1A blotted with anti-Rap1A (sc-1482) would be decreased. Surprisingly, non-geranylgeranylated Rap1A increased in OR6 cells after treatment with PTV and teprenone (compare lanes 3 and 7 in Fig. 6C). Furthermore, it is noteworthy that the total amount of Rap1 was decreased when OR6 cells were treated with PTV and teprenone. These results suggest that teprenone was not incorporated into host protein and unexpectedly enhanced the statin's inhibitory action against geranylgeranylation.

Teprenone enhanced statins' inhibitory action against geranylgeranylation

To further investigate the unexpected results shown in Figure 6C, we tested the geranylgeranyl state and anti-HCV activity using the OR6 assay system. OR6 cells were treated with teprenone (0, 10 and 20 μg/ml) in combination with PTV (0, 0.25, 0.5 and 1.0 μM) for 72 h and subjected to western blot analysis for the geranylgeranyl state using anti-Rap1A (sc-1482) and anti-Rap1 (sc-65) antibodies, and for anti-HCV activity using anti-Core, anti-NS5A and anti-NS5B antibodies. Anti-HCV activity was also assessed by a luciferase reporter assay. Teprenone by itself did not inhibit geranylgeranylation (lanes 1–3; Fig. 7A). When teprenone was treated with PTV (0.25 μM), nongeranylgeranylated Rap1A increased in a dose-dependent manner (lanes 4–6; Fig. 7A). This result indicates that teprenone enhanced PTV's inhibitory action against geranylgeranylation in a dose-dependent manner. This effect of teprenone was also confirmed when PTV was treated at concentrations of 0.5 and 1.0 μM (lanes 7–12; Fig. 7A). HCV RNA replication and the expression of HCV proteins were decreased when nongeranylgeranylated Rap1As were increased. Next, we examined whether or not this function of teprenone is a common feature against statins. Teprenone enhanced the inhibitory action of ATV, SIV, FLV and LOV but not PRV against geranylgeranylation (lower panel in Fig. 7B). Teprenone also enhanced anti-HCV activity in combination with statins (upper panel in Fig. 7B). These results

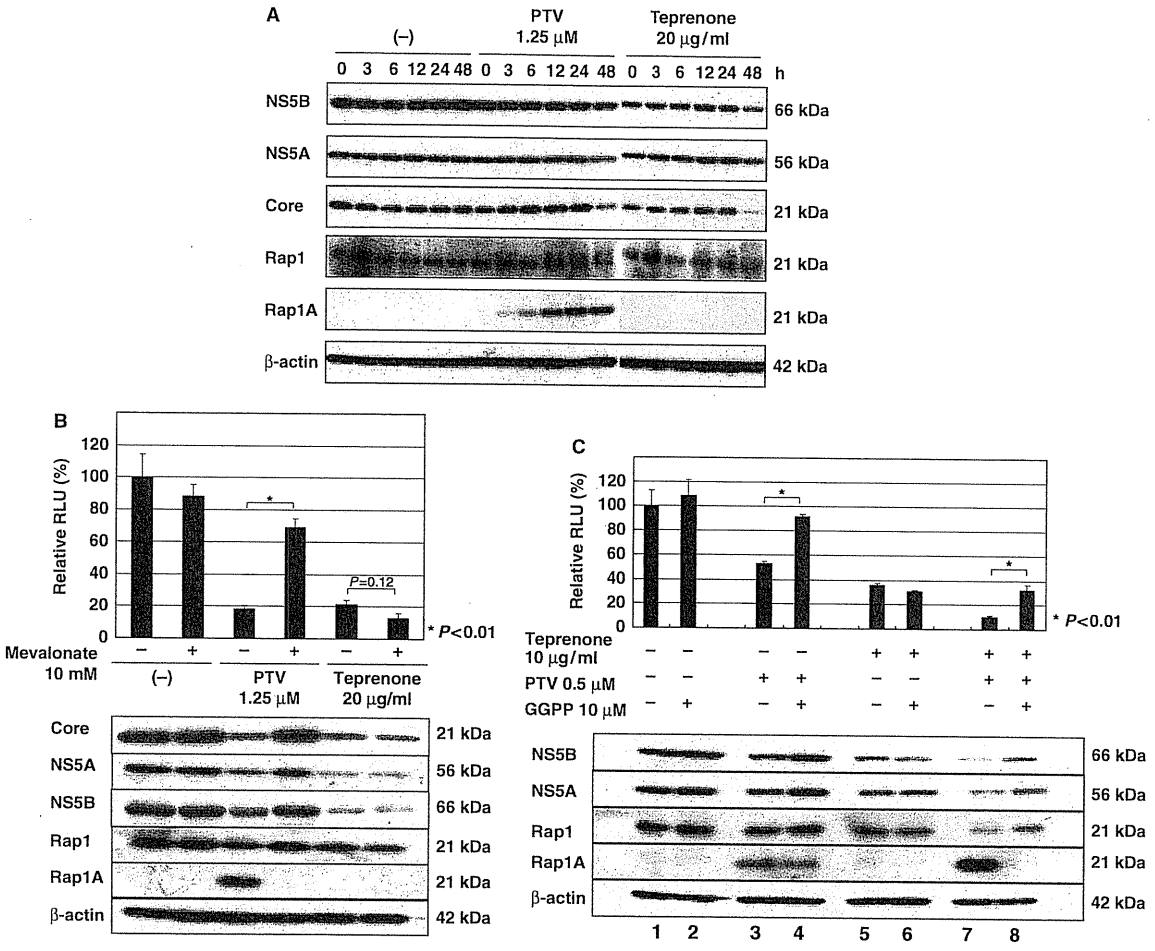

Fig. 6. Teprenone did not inhibit geranylgeranylation. (A) Teprenone did not inhibit geranylgeranylation. OR6 cells were treated with pitavastatin (PTV) (1.25 μM) or teprenone (20 μg/ml), or neither for 0, 3, 6, 12, 24 and 48 h. The cells were subjected to western blot analysis for HCV proteins using anti-NS5B, anti-NS5A and anti-Core antibodies, and for geranylgeranylation assay using anti-Rap1A (sc-1482) and anti-Rap1 (sc-65) antibodies. (B) Mevalonate did not affect the anti-HCV activity of teprenone. OR6 cells were treated with PTV (1.25 μM), teprenone (20 μg/ml) or neither in the absence or in the presence of mevalonate (10 mM) for 72 h. Then the cells were subjected to luciferase assay (upper panel) and western blot analysis using anti-Core, anti-NS5A, anti-NS5B, anti-Rap1A (sc-1482), anti-Rap1 (sc-65) and anti-β-actin antibodies (lower panel), as shown in (A). (C) Teprenone was not used as a substrate for GGT after the depletion of geranylgeranyl pyrophosphate (GGPP) by statin. OR6 cells were treated with teprenone (0 and 10 μg/ml), PTV (0 and 0.5 μM) and GGPP (0 and 10 μM) in the indicated combination for 72 h. Then the cells were subjected to luciferase assay (upper panel) and geranylgeranyl assay using anti-Rap1A (sc-1482) and anti-Rap1 (sc-65) antibodies (lower panel) as shown in (A).

suggest that teprenone enhances statins' inhibitory action against geranylgeranylation, except for PRV.

Discussion

In this study, we demonstrated that teprenone inhibited HCV RNA replication. Furthermore, teprenone exhibited anti-HCV activity in the genotype-2a JFH-1 infection system. Teprenone belongs to the geranyl compounds from its chemical structure and anti-ulcer agent from its clinical application. Therefore, we tested other geranyl compounds (GGOH and VK2, as well as geranylgeranoic acid) and other anti-ulcer agents (ecabet sodium, sofalcone and gefarnate) for their effect on HCV RNA replication. However, only teprenone exhibited anti-HCV activity among the reagents tested. Therefore, the anti-HCV activity of teprenone is a unique feature among these reagents.

The interview form from Selbex providing company Eisai reported the plasma concentration of teprenone. When 150 mg of Selbex was administered orally, its maximum plasma concentration reached 2.2 μg/ml. This is similar to the EC_{50} (5.3 μg/ml) of Selbex *in vitro*.

Ichikawa *et al.* (23) reported that teprenone induced the 2′,5′-oligoadenylate synthetases (2′5′-OAS) in

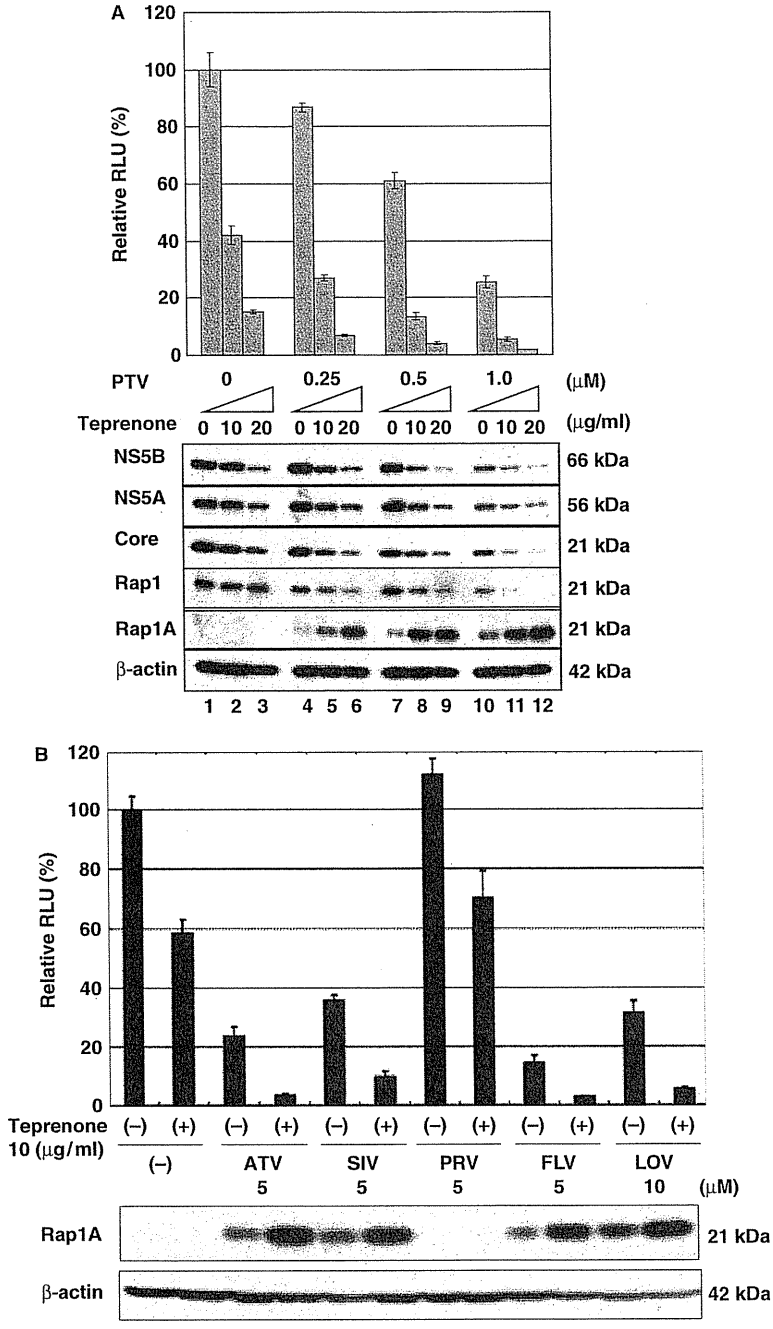

Fig. 7. Teprenone enhanced statins' inhibitory action against geranylgeranylation. (A) Teprenone enhanced pitavastatin (PTV)'s inhibitory action against geranylgeranylation. OR6 cells were treated with teprenone (0, 10 and 20 μg/ml) and PTV (0, 0.25, 0.5 and 1.0 μM) for 72 h. Then the cells were subjected to luciferase assay (upper panel) and western blot analysis using anti-NS5A, anti-Rap1A (sc-1482) and anti-Rap1 (sc-65), and anti-β-actin antibodies (lower panel), as shown in Figure 6A. (B) Teprenone enhanced statins' [except for pravastatin (PRV)] inhibitory action against geranylgeranylation. OR6 cells were treated with teprenone (0, 10 μg/ml) and atorvastatin (0, 5 μM), simvastatin (0, 5 μM), PRV (0, 5 μM), fluvastatin (0, 5 μM) and lovastatin (0, 10 μM) for 72 h. Then the cells were subjected to luciferase assay (upper panel) and western blot analysis using anti-Rap1A (sc-1482), and anti-β-actin antibodies (lower panel), as shown in Figure 6A.

Liver International (2011)

human hepatoma cells. We demonstrated the activation of 2′5′-OAS and IFN-stimulated response element (ISRE) by IFN-α using the reporter assay system in our HuH-7-derived OR6 cells. However, we could not obtain evidence that teprenone activated both 2′5′-OAS and ISRE promoters (supporting information, Fig. S2A and B). Signal transducer and activator of transcription (STAT)1 and STAT2 were not phosphorylated after treatment with teprenone (supporting information, Fig. S2C). This discrepancy may have been caused by the heterogeneity of HuH-7 cells, because OR6 was selected as the clonal cell line and is highly susceptible to HCV RNA replication. Further study is needed to clarify the mechanism underlying teprenone's effect on IFN signalling.

Teprenone reportedly protects the gastric mucosa by inducing HSP (24). From this standpoint, the anti-HCV activity of teprenone was an unexpected result, because recently, it was reported that HSP90 is essential for HCV RNA replication and that an HSP90 inhibitor, geldanamycin, inhibits HCV RNA replication (25, 26). We examined whether or not teprenone induced HSP90 in hepatoma cells and found that it did not (supporting information, Fig. S4).

In this study, we monitored the geranylgeranylated state of Rap1A as a marker using nongeranylgeranylated Rap1A-detectable anti-Rap1A antibody (sc-1482). The least expected result of this sensitive geranylgeranylation assay is that teprenone enhanced statins' inhibitory action against geranylgeranylation. It is not clear in this study as to why teprenone enhanced statins' inhibitory action on geranylgeranylation. One possibility is that teprenone may cause biosynthesis from FPP to cholesterol rather than to GGPP by an unknown mechanism. To clarify this point, further study will be needed. This new function of teprenone may contribute to not only the antiviral field but also other fields, including studies on osteoporosis and on various kinds of antitumours, because geranylgeranylation and farnesylation are targets of the reagent in these fields. For example, statins interfere with the production of GGPP and FPP, which is important in the activation of small G proteins, such as K-ras and the Rho family, and disrupt the growth of malignant cells.

Recently, two important findings have been reported. Firstly, El-Serag *et al.* (8) reported that statins are associated with a reduced risk of HCC. Secondly, Abraldes *et al.* (9) reported that statin lowers portal pressure in patients with cirrhosis. Therefore, as teprenone is a strong adjuvant to statin's inhibitory action against geranylgeranylation, it may further improve portal hypertension in cirrhosis and reduce the risk of HCC in combination with statins. Although teprenone alone possesses modest anti-HCV activity, it will play a significant role in combination with IFN and/or statins in the therapy to HCV-associated liver diseases as an adjuvant like ribavirin. As teprenone is available in clinical use with a low side effect, a clinical study using teprenone in combination with IFN-α and/or statins is now underway in our institution.

In conclusion, we have shown that the anti-ulcer agent teprenone inhibited HCV RNA replication and enhanced statins' inhibitory action against geranylgeranylation. This newly discovered function of teprenone may contribute to improve the treatment of HCV-associated liver diseases (CH C, cirrhosis and HCC) as an adjuvant to statins.

Acknowledgements

The authors would like to thank Atsumi Morishita, Takashi Nakamura and Midori Takeda for their technical assistance. This work was supported by grants-in-aid for a third-term comprehensive 10-year strategy for cancer control and for research on hepatitis from the Ministry of Health, Labor, and Welfare of Japan. K. A. and K. M. were supported by a Research Fellowship from the Japan Society for the Promotion of Science (JSPS) for Young Scientists.

References

1. Feld JJ, Hoofnagle JH. Mechanism of action of interferon and ribavirin in treatment of hepatitis C. *Nature* 2005; **436**: 967–72.
2. Ikeda M, Abe K, Dansako H, *et al.* Efficient replication of a full-length hepatitis C virus genome, strain O, in cell culture, and development of a luciferase reporter system. *Biochem Biophys Res Commun* 2005; **329**: 1350–9.
3. Ikeda M, Abe K, Yamada M, *et al.* Different anti-HCV profiles of statins and their potential for combination therapy with interferon. *Hepatology* 2006; **44**: 117–25.
4. Ikeda M, Kato N. Modulation of host metabolism as a target of new antivirals. *Adv Drug Deliv Rev* 2007; **59**: 1277–89.
5. Ikeda M, Kato N. Life style-related diseases of the digestive system: cell culture system for the screening of anti-hepatitis C virus HCV reagents: suppression of HCV replication by statins and synergistic action with interferon. *J Pharmacol Sci* 2007; **105**: 145–50.
6. Kim SS, Peng LF, Lin W, *et al.* A cell-based, high-throughput screen for small molecule regulators of hepatitis C virus replication. *Gastroenterology* 2007; **132**: 311–20.
7. Bader T, Fazili J, Madhoun M, *et al.* Fluvastatin inhibits hepatitis C replication in humans. *Am J Gastroenterol* 2008; **103**: 1383–9.
8. El-Serag HB, Johnson ML, Hachem C, Morgana RO. Statins are associated with a reduced risk of hepatocellular carcinoma in a large cohort of patients with diabetes. *Gastroenterology* 2009; **136**: 1601–8.
9. Abraldes JG, Albillos A, Banares R, *et al.* Simvastatin lowers portal pressure in patients with cirrhosis and portal hypertension: a randomized controlled trial. *Gastroenterology* 2009; **136**: 1651–8.

10. Kapadia SB, Chisari FV. Hepatitis C virus RNA replication is regulated by host geranylgeranylation and fatty acids. *Proc Natl Acad Sci USA* 2005; **102**: 2561–6.
11. Ye J, Wang C, Sumpter R Jr, *et al.* Disruption of hepatitis C virus RNA replication through inhibition of host protein geranylgeranylation. *Proc Natl Acad Sci USA* 2003; **100**: 15865–70.
12. Wang C, Gale M Jr, Keller BC, *et al.* Identification of FBL2 as a geranylgeranylated cellular protein required for hepatitis C virus RNA replication. *Mol Cell* 2005; **18**: 425–34.
13. Lindenbach BD, Evans MJ, Syder AJ, *et al.* Complete replication of hepatitis C virus in cell culture. *Science* 2005; **309**: 623–6.
14. Wakita T, Pietschmann T, Kato T, *et al.* Production of infectious hepatitis C virus in tissue culture from a cloned viral genome. *Nat Med* 2005; **11**: 791–6.
15. Zhong J, Gastaminza P, Cheng G, *et al.* Robust hepatitis C virus infection in vitro. *Proc Natl Acad Sci USA* 2005; **102**: 9294–9.
16. Nanke Y, Kotake S, Ninomiya T, *et al.* Geranylgeranylacetone inhibits formation and function of human osteoclasts and prevents bone loss in tail-suspended rats and ovariectomized rats. *Calcif Tissue Int* 2005; **77**: 376–85.
17. Kato N, Sugiyama K, Namba K, *et al.* Establishment of a hepatitis C virus subgenomic replicon derived from human hepatocytes infected in vitro. *Biochem Biophys Res Commun* 2003; **306**: 756–66.
18. Naka K, Ikeda M, Abe K, Dansako H, Kato N. Mizoribine inhibits hepatitis C virus RNA replication: effect of combination with interferon-alpha. *Biochem Biophys Res Commun* 2005; **330**: 871–9.
19. Dansako H, Naganuma A, Nakamura T, *et al.* Differential activation of interferon-inducible genes by hepatitis C virus core protein mediated by the interferon stimulated response element. *Virus Res* 2003; **97**: 17–30.
20. Ariumi Y, Kuroki M, Abe K, *et al.* DDX3 DEAD-box RNA helicase is required for hepatitis C virus RNA replication. *J Virol* 2007; **81**: 13922–6.
21. Hughes A, Rogers MJ, Idris AI, Crockett JC. A comparison between the effects of hydrophobic and hydrophilic statins on osteoclast function in vitro and ovariectomy-induced bone loss in vivo. *Calcif Tissue Int* 2007; **81**: 403–1.
22. Merrell MA, Wakchoure S, Lehenkari PP, Harris KW, Selander KS. Inhibition of the mevalonate pathway and activation of p38 MAP kinase are independently regulated by nitrogen-containing bisphosphonates in breast cancer cells. *Eur J Pharmacol* 2007; **570**: 27–37.
23. Ichikawa T, Nakao K, Nakata K, *et al.* Geranylgeranylacetone induces antiviral gene expression in human hepatoma cells. *Biochem Biophys Res Commun* 2001; **280**: 933–9.
24. Hirakawa T, Rokutan K, Nikawa T, Kishi K. Geranylgeranylacetone induces heat shock proteins in cultured guinea pig gastric mucosal cells and rat gastric mucosa. *Gastroenterology* 1996; **111**: 345–57.
25. Nakagawa S, Umehara T, Matsuda C, *et al.* Hsp90 inhibitors suppress HCV replication in replicon cells and humanized liver mice. *Biochem Biophys Res Commun* 2007; **353**: 882–8.
26. Okamoto T, Nishimura Y, Ichimura T, *et al.* Hepatitis C virus RNA replication is regulated by FKBP8 and Hsp90. *Embo J* 2006; **25**: 5015–25.

Supporting information

Additional supporting information may be found in the online version of this article:

Fig. S1. The effects of anti-ulcer agents on HCV RNA replication. (A) Cell proliferation assay. OR6 cells were treated with teprenone (0, 2.5, 5, 10, and 20 μg/ml), and the cells at 24, 48, and 72 hours after treatment were subjected to WST-1 cell proliferation assay. (B) Structures of ant-ulcer agents. (C-E) OR6 cells were treated with ecabet sodium (0, 2.5, 5, 10, 20 μg/ml) (C), sofalcon (0, 2.5, 5, 10, 20 μg/ml) (D), and gefarnate (0, 2.5, 5, 10, 20 μg/ml) (E) for 72 hours. Then the cells were subjected to luciferase assay (upper panel) and Western blot analysis using anti-core, and anti-β-actin antibodies (lower panel) as shown in Figure 1B.

Fig. S2. Teprenone didn't activate IFN signaling pathway. (A and B) Luciferase assays for 2'5'OAS and ISRE promoters. p2'5'OAS-luc (A) and pISRE-luc (B) transfected OR6c cells were treated with teprenone (0, 2.5, 5, and 10 μg/ml) or IFN-α (0, 2.5, 5, and 10 IU/ml) for 6 hours and then subjected to luciferase reporter assay. (C) Teprenone didn't activate STATs in OR6 cells. OR6 cells were treated with IFN-α (500 IU/ml), PTV (1.25 μM), and teprenone (20 μg/ml) for 0, 3, 6, and 12 hours. Then the cells were subjected to Western blot analysis using anti-pSTAT1 (Tyr701), anti-STAT1, anti-pSTAT2 (Tyr689), anti-core, and anti-β-actin antibodies.

Fig. S3. Teprenone treatment didn't cause positive feedback of HMG-CoA reductase (HMGCR). OR6c cells were treated with teprenone (20 μg/ml), PTV (10 μmol/L), or neither for 24 hours. The cells were subjected to RT-PCR (A) and real-time RT-quantitative PCR (B) using HMG-CoA reductase-specific primer set. H_2O was used as a negative control. GAPDH was used as an internal control.

Fig. S4. Teprenone didn't induce HSP90 or HSP70 in HuH-7 cells. OR6 cells were treated with teprenone (20 μg/ml) for 0, 3, 6, 12, 24, and 48 hours. Then the cells were subjected to Western blot analysis using anti-HSP90, anti-HSP70 anti-core, and anti-β-actin antibodies.

Please note: Wiley-Blackwell is not responsible for the content or functionality of any supporting materials supplied by the authors. Any queries (other than missing material) should be directed to the corresponding author for the article.

Virus Research 157 (2011) 61–70

Contents lists available at ScienceDirect

Virus Research

journal homepage: www.elsevier.com/locate/virusres

Mechanism of action of ribavirin in a novel hepatitis C virus replication cell system

Kyoko Mori[a], Masanori Ikeda[a], Yasuo Ariumi[a], Hiromichi Dansako[a], Takaji Wakita[b], Nobuyuki Kato[a,*]

[a] Department of Tumor Virology, Okayama University Graduate School of Medicine, Dentistry, and Pharmaceutical Sciences, 2-5-1 Shikata-cho, Okayama 700-8558, Japan
[b] Department of Virology II, National Institute of Infectious Diseases, 1-23-1 Toyama, Shinjuku-ku, Tokyo 162-8640, Japan

ARTICLE INFO

Article history:
Received 16 November 2010
Received in revised form 4 February 2011
Accepted 4 February 2011
Available online 12 February 2011

Keywords:
HCV
HCV RNA replication system
RBV
IMPDH inhibitor

ABSTRACT

Ribavirin (RBV) is a potential partner of interferon (IFN)-based therapy for patients with chronic hepatitis C. However, to date, its anti-hepatitis C virus (HCV) mechanism remains ambiguous due to the marginal activity of RBV on HCV RNA replication in HuH-7-derived cells, which are currently used as the only cell culture system for robust HCV replication. We investigated the anti-HCV activity of RBV using novel cell assay systems. The recently discovered human hepatoma cell line, Li23, which enables robust HCV replication, and the recently developed Li23-derived drug assay systems (ORL8 and ORL11), in which the genome-length HCV RNA (O strain of genotype 1b) encoding renilla luciferase efficiently replicates, were used for this study. At clinically achievable concentrations, RBV unexpectedly inhibited HCV RNA replication in ORL8 and ORL11 systems, but not in OR6 (an HuH-7-derived assay system). The anti-HCV activity of RBV was almost cancelled by an inhibitor of equilibrative nucleoside transporters. The evaluation of the anti-HCV mechanisms of RBV proposed to date using ORL8 ruled out the possibility that RBV induces error catastrophe, the IFN-signaling pathway or oxidative stress. However, we found that the anti-HCV activity of RBV was efficiently cancelled with guanosine, and demonstrated that HCV RNA replication was notably suppressed in inosine monophosphate dehydrogenase (IMPDH)-knockdown cells, suggesting that the antiviral activity of RBV is mediated through the inhibition of IMPDH. In conclusion, we demonstrated for the first time that inhibition of IMPDH is a major antiviral target by which RBV at clinically achievable concentrations inhibits HCV RNA replication.

1. Introduction

Hepatitis C virus (HCV) infection causes chronic hepatitis, which often leads to liver cirrhosis and hepatocellular carcinoma (Thomas, 2000). Since approximately 170 million people are infected with HCV worldwide, HCV infection is a serious global health problem (Thomas, 2000). HCV is an enveloped positive single-stranded RNA virus of the *Flaviviridae* family. The HCV genome encodes a large polyprotein precursor of approximately 3000 amino acids, which is cleaved into in the following order: Core, envelope 1 (E1), E2, p7, non-structural protein 2 (NS2), NS3, NS4A, NS4B, NS5A, and NS5B (Kato et al., 1990).

The current standard therapy for patients with chronic hepatitis C is a combination of pegylated-interferon (PEG-IFN) and ribavirin (RBV). This treatment currently achieves a sustained virological response (SVR) greater than 50% (Chevaliez et al., 2007). However, the mechanism of RBV activity in patients with chronic hepatitis C is still ambiguous. To date, five distinct mechanisms have been proposed: (a) RBV acts as an RNA mutagen that causes mutations of the HCV RNA genome and induces a so-called "error catastrophe" (Feld and Hoofnagle, 2005); (b) RBV enhances the IFN-signaling pathway (Feld et al., 2010; Thomas et al., 2011); (c) RBV induces GTP depression by inhibiting inosine monophosphate dehydrogenase (IMPDH) (Zhou et al., 2003); (d) RBV directly inhibits NS5B-encoded RNA-dependent RNA polymerase (Feld and Hoofnagle, 2005); (e) RBV enhances host T-cell mediated immunity by switching the T-cell phenotype from type 2 to type 1 (Lau et al., 2002). Unfortunately, no groups have clarified the anti-HCV mechanism of RBV at clinically achievable concentrations (5–14 μM) (Feld et al., 2010; Pawlotsky et al., 2004; Tanabe et al.,

Abbreviations: HCV, hepatitis C virus; E1, envelope 1; NS2, nonstructural protein 2; PEG, polyethylene glycol; IFN, interferon; RBV, ribavirin; SVR, sustained virological response; IMPDH, inosine monophosphate dehydrogenase; RL, renilla luciferase; EC_{50}, 50% effective concentration; VE, vitamin E; NBMPR, *S*-(4-nitrobenzyl)-6-thioinosine; MPA, mycophenolic acid; CsA, cyclosporine A; STAT1, signal transducer and activator of transcription 1; ENT, equilibrative nucleoside transporter; RT-PCR, reverse-transcription polymerase chain reaction; ISG, IFN-stimulated gene; IRF7, IFN regulatory factor 7; IP-10, IFN-gamma-inducible protein-10; GAPDH, glyceraldehyde-3-phosphate dehydrogenase; 5′-UTR, 5′-untranslated region; Neo^R, neomycin-resistance gene; CNT, concentrative nucleoside transporter; EC_{90}, 90% effective concentration; CFE, colony-forming efficiency; MMPD, merimepodib.

* Corresponding author. Tel.: +81 86 235 7385; fax: +81 86 235 7392.
E-mail address: nkato@md.okayama-u.ac.jp (N. Kato).

0168-1702/$ – see front matter © 2011 Elsevier B.V. All rights reserved.
doi:10.1016/j.virusres.2011.02.005

2004). Although most of the above mechanisms were proposed based on studies using HuH-7 (human hepatoma cell line)-derived cells, which are currently used as the only cell culture system for robust HCV replication, the effective concentrations (50–1000 μM) of RBV were much higher than the clinically achievable concentrations (Feld and Hoofnagle, 2005; Feld et al., 2010; Lau et al., 2002; Pawlotsky et al., 2004; Thomas et al., 2011; Zhou et al., 2003). Indeed, our HuH-7-derived cell assay system (OR6) (Ikeda et al., 2005; Naka et al., 2005), in which genome-length HCV RNA (O strain of genotype 1b) encoding renilla luciferase (RL) efficiently replicates, also showed that the 50% effective concentration (EC_{50}) of RBV was approximately 100 μM (Naka et al., 2005).

Recently, we found a new human hepatoma cell line, Li23, that enables robust HCV RNA replication (Kato et al., 2009). We showed by microarray analysis that Li23 cells possessed expression profiles rather different from those in HuH-7 cells (Kato et al., 2009), and that the expression profile of Li23 cells was distinct from those of frequently used other hepatoma cell lines (Mori et al., 2010). We further developed Li23-derived cell culture assay systems (ORL8 and ORL11) in which genome-length HCV RNA (O strain of genotype 1b) encoding RL efficiently replicates (Kato et al., 2009). Here, we unexpectedly observed through the use of these cell culture assay systems the first evidence of anti-HCV activity of RBV at clinically achievable concentrations, and obtained the convincing data that the anti-HCV mechanism of RBV is mediated through the inhibition of IMPDH.

2. Materials and methods

2.1. Cell cultures

HuH-7-derived cells harboring an HCV replicon or genome-length HCV RNA were maintained with medium containing G418 (0.3 mg/ml) as described previously (Ikeda et al., 2005). Li23-derived polyclonal sORL8 and sORL11 cells harboring an HCV replicon were established by the transfection of ORN/3-5B/QR,KE,SR RNA (Kato et al., 2009) into the cured OL8 and OL11 cells, respectively. Li23-derived cells harboring an HCV replicon or genome-length HCV RNA were maintained as described previously (Kato et al., 2009). Cured cells, from which the HCV RNA had been eliminated by IFN treatment, were also maintained as described previously (Kato et al., 2009).

2.2. RL assay

RL assay was performed as described previously (Ikeda et al., 2005; Kato et al., 2009). The experiments were performed at least in triplicate.

2.3. Reagents

RBV was kindly provided by Yamasa (Chiba, Japan). Human IFN-α, vitamin E (VE), phloridzin dihydrate, *S*-(4-nitrobenzyl)-6-thioinosine (NBMPR), and mycophenolic acid (MPA) were purchased from Sigma–Aldrich (St. Louis, MO). Cyclosporine A (CsA) was purchased from Calbiochem (San Diego, CA). Guanosine and adenosine were purchased from Wako Pure Chemical Industries, Ltd. (Osaka, Japan).

2.4. Cell viability

Cell viability was examined by the method described previously (Kato et al., 2009). The experiments were performed in triplicate.

2.5. Western blot analysis

The preparation of cell lysates, sodium dodecyl sulfate–polyacrylamide gel electrophoresis and immunoblotting analysis with a PVDF membrane were performed as previously described (Kato et al., 2003). The antibodies used in this study were those against Core (CP11; Institute of Immunology, Tokyo, Japan), NS5B (a generous gift from Dr. M. Kohara, Tokyo Metropolitan Institute of Medical Science), signal transduction and activator of transcription 1 (STAT1) and phospho-STAT1 (Tyr701) (BD Transduction Laboratories, Lexington, KY) and equilibrative nucleoside transporter 1 (ENT1) (Abgent, San Diego, CA). β-actin antibody (Sigma–Aldrich) was used as the control for the amount of protein loaded per lane. Immunocomplexes were detected by using a Renaissance enhanced chemiluminescence assay (Perkin Elmer Life Sciences, Boston, MA).

2.6. Reverse transcription-polymerase chain reaction (RT-PCR)

Total RNA from the cultured cells was extracted with an RNeasy Mini Kit (Qiagen, Valencia, CA). RT-PCR was performed by a method described previously (Dansako et al., 2003) using the following primer pairs: IFN-stimulated gene (ISG) 15 (346 bp), 5′-GCCTTCCAGCAGCGTCTGGC-3′ and 5′-GCAGGCGCAGATTCATGAACACGG-3′; IFN regulatory factor 7 (IRF7) (221 bp), 5′-AGCTGCGCTACACGGAGGAACTG-3′ and 5′-CCACCAGCTCTTGGAAGAAGAC-3′; IFN-gamma-inducible protein-10 (IP-10) (111 bp), 5′-GGCCATCAAGAATTTACTGAAAGCA-3′ and 5′-TCTGTGTGGTCCATCCTTGGAA-3′; ENT1 (382 bp), 5′-GAGTTTCA-GTCTCCAACTCTCAG-3′ and 5′-GCATCGTGCTCGAAGACCACAG-3′; ENT2 (306 bp), 5′-CTTGTGTTGGTCTTCACAGTCAC-3′ and 5′-GGTGATGAAGTAGGCATCCTGTG-3′; ENT3 (350 bp), 5′-GTCTTCTTCATCACCAGCCTCATC-3′ and 5′-GTGCTGAGGTAGCCGT-TGCTGAG-3′; glyceraldehyde-3-phosphate dehydrogenase (GAPDH) (334 bp), 5′-GACTCATGACCACAGTCCATGC-3′ and 5′-GAGGAGACCACCTGGTGCTCAG-3′.

2.7. Infection of cells with secreted HCV

The inoculum was prepared from HCV-JFH1 (Wakita et al., 2005)-infected HuH-7-derived RSc cells (Ariumi et al., 2007; Kato et al., 2009) at 5 days postinfection and then stored at −80 °C after filtering through a 0.20-μm filter (Kurabo, Osaka, Japan) until use. ORL8c or RSc cells (each 5×10^4) were cultured for 24 h before infection. The cells were infected with 50 μl (equivalent to a multiplicity of infection of 0.05–0.1) of inoculum and maintained for several days until RBV treatment.

2.8. Quasispecies analysis of HCV RNA

ORL8 cells were treated with or without RBV (50 μM) for 72 h. Total RNA from the cultured cells was extracted with an RNeasy Mini Kit (Qiagen). To amplify genome-length HCV RNA, RT-PCR was performed separately in two fragments using KOD-plus DNA polymerase (Toyobo) as described previously (Ikeda et al., 2005; Kato et al., 2003). The two PCR products (the 6.0 kb region covering 5′-untranslated region (5′-UTR) to NS3 and the 6.1 kb region covering NS2 to NS5B) were subcloned into the *Xba*I site of pBR322MC, and sequence analysis of the region encoding RL to the neomycin-resistance gene (Neo^R) (1953 nts), NS5A (1341 nts), or NS5B (1773 nts) was performed as described previously (Ikeda et al., 2005). Synonymous and nonsynonymous substitutions at variance with the parental ORN/C-5B/QR,KE,SR sequences (Kato et al., 2009) were determined. To examine the error frequency of KOD-plus DNA polymerase in the PCR amplification, PCR using the plasmid containing ORN/C-5B/QR,KE,SR sequences was performed separately in the